

Reviewed Preprint

v1 • October 31, 2025

Not revised

Reviewed Preprint

v2 • June 22, 2026

Revised by authors

✉ For correspondence:

c.alonso@sussex.ac.uk

Competing interests: No

competing interests declared

Funding: See [page 27](#)

Reviewing editor: Sonia Sen, Tata

Institute for Genetics and Society,

India

© 2025, Roseby et al. This article is distributed under the terms of the [Creative Commons Attribution License](#), which permits unrestricted use and redistribution provided that the original author and source are credited.

Region-specific mechanosensation modulates *Drosophila* postural control behaviour

William Roseby, Jonathan AC Menzies, Victoria A Lipscomb, Claudio R Alonso ✉

Department of Neuroscience, Sussex Neuroscience, School of Life Sciences, University of Sussex, Brighton, United Kingdom

eLife Assessment

This study by Roseby and colleagues shows that region-specific mechanosensation - especially anterior-dorsal inputs - controls larval self-righting, and links this to Hox gene function in sensory neurons. The work is **important** for understanding how body plan cues shape sensorimotor behaviour, and the experimental toolkit will be of use to others. The strength of evidence is **compelling** with respect to the assays developed and the involvement of the anterior region, the evidence is more limited with respect to the dorso-ventral organization of sensory inputs in that region and the mechanism by which Hox genes contribute to the process. These findings will be of broad interest to researchers studying neural circuits, developmental genetics, and the evolution of behaviour.

<https://doi.org/10.7554/eLife.108505.2.sa3>

Abstract

The relation between regional morphological features derived from the bilaterian body plan and the behaviours necessary to extract utility from such structures is not well understood. Here we use the *Drosophila* larva to investigate this ‘form-function’ problem focusing on the mapping of the regional stimuli that trigger an adaptive and evolutionarily conserved behaviour termed self-righting: a postural control system that allows the animal to restore its natural position if turned upside-down. Through the development of new methodologies that allow regionally-restricted mechanical stimulation and zonal-specific neuronal optogenetics, we find that multidendritic sensory neuron inhibition in anterior areas (thoracic/anterior abdominal) has a profound effect on self-righting performance, whilst inhibition of posterior sensory elements (mid and posterior abdomen) produces no effects. To gain insight into how regional neuronal inhibition affects the different subcomponents of the self-righting sequence we applied a deep neural network tracking method which revealed that reduction of neural activity in anterior sensory neurons primarily increases head casting behaviour, and that this, in turn, is strongly correlated with abnormally long self-righting times. Furthermore, to explore the mechanistic bases of our behavioural observations, we considered the hypothesis that the *Hox* genes – well known for their roles in axial developmental patterning – might play a role in the functional specification of multidendritic sensory neurons along the body axis. Molecular expression analysis of FACS-sorted neural populations, fluorescent immunolabelling and neuron-specific knock-down experiments demonstrate that normal sensory neuron expression of the *Hox* genes *Antennapedia* and *Abdominal-b* is necessary for self-righting in the *Drosophila* larva. Altogether, our work shows that region-specific mechanosensory processes mediated by multidendritic sensory neurons and instructed via *Hox* gene inputs are essential for self-righting, providing a link between regional structural features and an adaptive and widely evolutionarily conserved postural control behaviour.

Introduction

Bilaterally symmetric animals (Bilateria) represent the largest group of animals, including highly diverse phyla such as Arthropoda and Chordata. The bilaterian *bauplan* derives from the last common ancestor to all bilaterians, the urbilaterian [De Robertis & Sasai, 1996], which is believed to have possessed a substantial level of complexity featuring a nervous system, and a regionalised main body axis running from head-to-tail (antero-posterior, AP axis) as well as an orthogonal axis, the dorsoventral (DV) axis. Urbilaterians are thought to have lived in the ocean with a pelagic larval form and a benthic adult inhabiting the sea bottom, crawling around and burrowing in the rich nutritional environment provided by phytoplankton sediments [De Robertis & Tejada-Muñoz, 2022].

Several functional features present in modern bilaterians are linked to the axial organisation derived from the urbilaterian AP and DV coordinates. For example, the anterior region in most bilaterians hosts arrays of sensory organs – eyes, olfactory and gustatory systems, and so on – all located in close proximity to the brain, presumably with the dual purpose of detecting new information as quickly as it is received when the animal moves forward and enters new environments, and to save ‘on wire’ and speed-up information transfer [Sterling and Laughlin, 2015]. Another salient feature is that the ventral side of the body is often specialised for contact with the substrate (or medium) through cilia, protruding appendages, limbs, or, simply equipped with morphological elements that provide some form of ‘grip’ or means to propel the animal forward as it moves around its habitat.

Nonetheless, for all these morphological specialisations to contribute to fitness, the animal must be capable of generating a suitable behavioural repertoire to safeguard an adequate body orientation in the face of unexpected environmental change. An example of this type of behaviour is a common postural control system termed *self-righting* [Picao-Osorio et al., 2015], which allows the animal to restore its normal orientation in respect to substrate should it find itself ‘upside-down’ [Figure 1A]. Self-righting is evolutionarily conserved all the way from insects to mammals [Ashe, 1970; Penn, 1995; Faisal & Matheson 2005; Jusufi et al., 2011; Feather-Schussler & Ferguson, 2016; Bagnall & Schoppik, 2018] [Figure 1B], including humans where it constitutes an element of medical tests evaluating motor development in young infants [McGraw, 1941; Teitelbaum et al., 1998; Siegel et al., 2024]. Notably, the relation between regional internal/external structural features derived from body plan organisation and the simple behaviours necessary to extract functionality from such elaborated structural features is not well understood. Here we study this ‘form-function’ problem in the *Drosophila* larva seeking to determine the signals that trigger self-righting and how such signals relate to body plan organisation and morphology.

Previous work demonstrated that all motile developmental stages of the fruit fly display self-righting, including the three larval stages and the adult [Issa et al., 2021]; of these, the larval stage is probably the simplest to advance the question on stimulation given the lower morphological and neural complexity of the larva compared to adult forms. Further work identified several genetic elements essential for self-righting via activities in the sensory and motor domains [Picao-Osorio et al 2015; Picao-Osorio et al 2015; Issa et al. 2019; Klann et al. 2021]. Despite this progress, the signals that prompt the self-righting response remain largely unknown, except from the fact that gravity does not play a role [Klann et al., 2021].

To determine the stimuli that trigger larval self-righting we first developed a new approach that allows a precise temporal and quantitative analysis of self-righting responses, the ‘water unlocking technique’. Using this new technique in a series of combinatorial mechanical stimulation experiments providing specific surface contacts on the anterior, posterior, ventral and/or dorsal sides of the larva (and combinations therewith) we discover that for self-righting to occur the animal requires anterior dorsal contact in the absence of ventral anterior contact. Seeking to advance the understanding of the cellular processes that underlie the triggering of self-righting, we considered the possibility that sensory neurons might play a role; to test this, we conditionally inhibited different subpopulations of larval sensory neurons using a thermogenetic

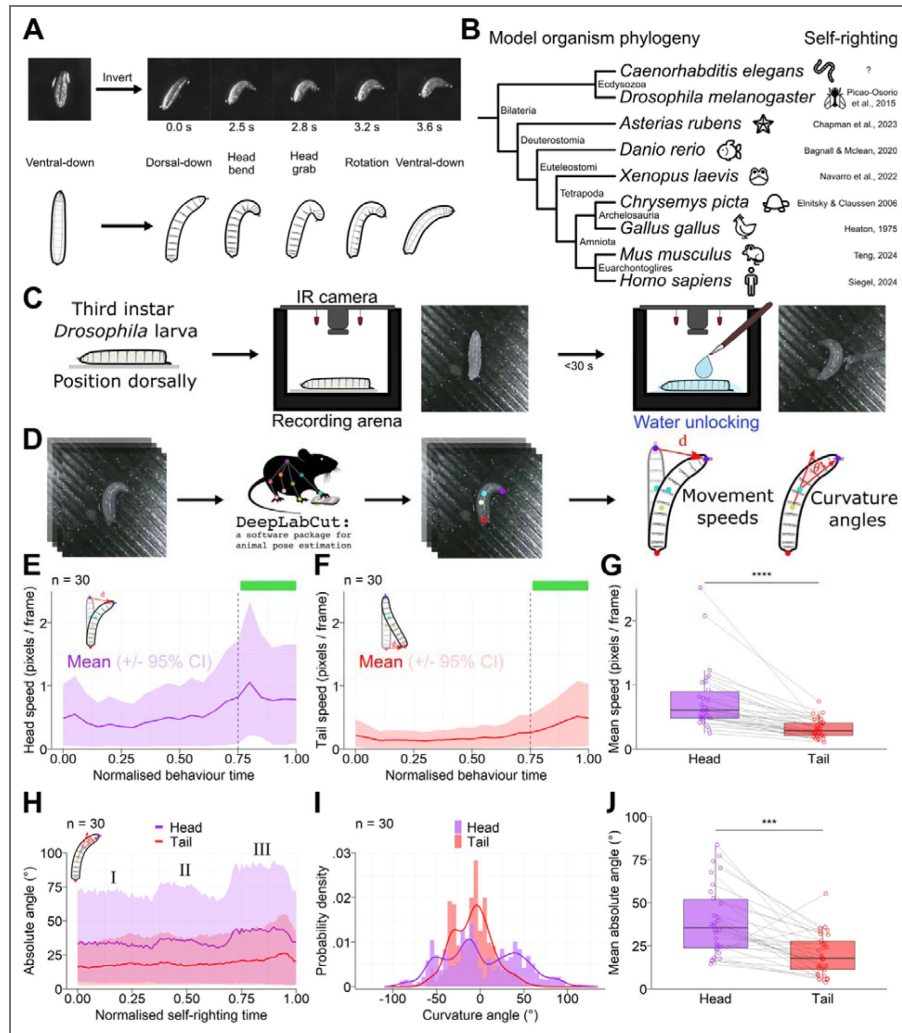


Figure 1. Quantitative analysis of self-righting behaviour

(A) Photographs (top) and diagrams (bottom) of the self-righting sequence of a first-instar *Drosophila* larva. After inversion of the normal posture, the self-righting sequence involves a 180° rotation of the body that begins at the head and takes around 3-5 seconds on average. (B) A phylogenetic tree of common model organisms, with a reference to documented self-righting behaviour on the right. (C) Experimental procedure for consistent recording of self-righting behaviour. Third-instar *w¹¹¹⁸* larvae were positioned on a dry coverslip with the dorsal side in contact with the surface before being placed in an arena for recording. Behaviour was ‘unlocked’ at the desired moment through the application of water with a moistened paintbrush. (D) Extraction of behavioural features with video tracking. Video frames were analysed using DeepLabCut, where four points along the anterior-posterior axis were labelled. The coordinates of these points were used to calculate speed of movement as well as angles of body curvature. (E) Mean head speed and (F) tail speed over the course of recordings. The lines show the mean taken over all samples while the shaded areas indicate the 95% CI. The time course has been normalised to account for differences in the length of behaviour. The dotted line in E indicates where the self-righting sequence is predicted to begin on average, based on head movement. (G) Mean speed of movement for the head and tail during the self-righting sequence. Points indicate mean speeds for individual samples, with measurements from the same larva being connected by lines. The box and whisker plots indicate the median, IQR and 1.5 IQR. ‘****’ = $P < 0.001$ for Wilcoxon signed rank tests, $n = 30$. (H) Absolute angles of curvature of the head (purple) and tail (red) over the course of the self-righting sequence. The lines show the mean absolute angle while the shaded areas indicate the 95% CI. Due to the apparent curvature of the head in three discrete bursts, the head angles have been labelled I, II and III. (I) The distribution of curvature angles for the head (purple) and tail (red), where negative values are left-handed bends and positive values are right-handed bends. The lines show a smoothed kernel density estimation for the probability density while the bars indicate counts binned to each 10°. (J) Mean absolute angle for the head and tail during the self-righting sequence. Points indicate mean speeds for individual samples, with measurements from the same larva being connected by lines. The box and whisker plots indicate the median, IQR and 1.5 IQR. ‘***’ = $P < 0.001$ for Wilcoxon signed rank tests, $n = 30$. The median self-righting times before and after trimming based on head movement were 12.8 and 11.0 seconds respectively.

approach and determined that normal sensory neuron activity – in particular that of multidendritic sensory neurons – is required for normal larval self-righting to occur. Building on these observations, we developed another specialised approach – the ‘opto-axial method’ – which allows regional-specific optogenetic manipulation of sensory neurons located at different axial positions of the larva. Using the opto-axial approach we established that multidendritic sensory neuron inhibition in anterior areas (thoracic and anterior abdominal) has a profound effect on self-righting performance; in contrast, inhibition of posterior sensory elements (mid and posterior abdomen) has no noticeable impact on self-righting. Targeted application of this method shows the md subpopulation of daIVs also follows the axial pattern, albeit with reduced effect size compared to the entire md population. Exploring the genetic basis underlying these differential role of axial sensory neurons we explored the possibility that the Hox genes – known for their roles in axial developmental patterning [Mallo and Alonso, 2013 [↗](#)] – might play a role; for this, we first demonstrated Hox expression in multidendritic sensory neurons, and, secondly, showed that normal sensory neuron expression of the Hox genes *Antennapedia* and *Abdominal-b* is necessary for “normal” self-righting in the *Drosophila* larva.

Altogether our work demonstrates that region-specific mechanosensory processes mediated by multidendritic sensory neurons and Hox gene inputs are essential for self-righting providing a link between regional internal structural features and an adaptive and widely evolutionarily conserved postural control behaviour. Based on the phylogenetic conservation of self-righting we propose that it may have been an ancestral behaviour present in the urbilaterian, suggesting that similar regional mechanosensory processes might play an important role in the triggering of self-righting in other animal systems.

Materials and methods

Fly stocks and maintenance

All fly stocks were reared on standard molasses food at 25 °C and 45% relative humidity, with a day-night cycle of 12:12. For experiments involving embryos or first instar larvae, stocks were transferred to a cage with an apple juice agar plate supplemented with yeast paste and samples were collected from the plate. For experiments with third instar larvae, samples were collected directly from the molasses food and briefly rinsed in water before being transferred to a 1% plain agar plate. To generate larvae for optogenetic experiments, crosses were carried out directly in molasses food supplemented with ATR. Most stocks were acquired from the Bloomington *Drosophila* Stock Centre (BDSC). For a full list of stocks used in this study, see [Table 1 \[↗\]\(#\)](#) below.

Behavioural assays

Unless otherwise stated, all behavioural experiments were conducted at an ambient temperature of 25.0 (+/- 1.0 °C) and a relative humidity between 40 and 60%. All experiments were conducted during a window of zeitgeber time ZT4-ZT8 (NB: ZT0 = lights turn on; ZT12 = lights off). Equal numbers of control and experimental larvae were tested under the same conditions on the same day, excluding occasional larvae that were discarded during the course of an experiment. Larvae were not distinguished by sex, so any sample was assumed to be a random mix of two sexes. For consistency between experimental setups, completion of self-righting behaviour was taken to be the time between experimental manipulation (e.g., water application), and the first moment when both tracheal trunks were visible along the whole length of the larva. Similarly, for completion of crawling, this was the time from experimental manipulation to completion of a peristaltic wave from posterior to anterior. Behavioural recordings were captured with a USB infrared CMOS camera (2MP OV2710, Arducam Technology Co. Ltd, Hong Kong) recording at 30 fps at 1920 × 1080. Behavioural arenas were 3D-printed in black PLA (1.75mm, RS Pro, UK) using a Prusa MK3S (Prusa Research, Czech Republic), with a layer height of 0.2 mm and 15% infill.

Stock	Source	Reference
<i>w¹¹¹⁸</i>	Alonso lab	Hazelrigg et al., 1984
<i>yw</i>	Alonso lab	Nash and Yarkin, 1974
<i>yw; 109(2)80-Gal4</i>	BDSC #8769	Gao et al., 1999
<i>yw; 109(2)80-Gal4, UAS-mCD8::GFP</i>	BDSC #8768	Gao et al., 1999

Table 1. List of *Drosophila* stocks used in this study.

<i>yw;; nompC-Gal4</i>	VDRC 2054	Yan et al. 2013
<i>w;; ppk-Gal4</i>	BDSC #32079	Ainsley et al. 2003
<i>w;; UAS-shi^[ts]</i>	BDSC #44222	Kitamoto, 2001
<i>w; UAS-GtACR2</i>	BDSC #92984	Govorunova et al., 2015
<i>w;; 10XUAS-GCaMP6s::tdTomato</i>	Marta Zlatic	Grover et al., 2020
<i>yv;; UAS-Antp- Valium10-RNAi</i>	BDSC #27675	Perkins et al., 2015
<i>yv;; UAS-Ubx- Valium10-RNAi</i>	BDSC #31913	Perkins et al., 2015
<i>yv;; UAS-AbdA- Valium10-RNAi</i>	BDSC #28739	Perkins et al., 2015
<i>yv;; UAS-AbdB- Valium10-RNAi</i>	BDSC #26746	Perkins et al., 2015
<i>yw;; UAS-Valium10-GFP</i>	BDSC #35786	Perkins et al., 2015

Table 1. (continued)

Water unlocking technique

For several experiments, we required a method of controlling larval position and restricting movement prior to beginning a behavioural test. We developed a technique centred around the presence of moisture, which is required for larval movement. We restricted movement by first drying larvae on a soft tissue, then subsequently transferring them to a standard microscope coverslip (22 × 22 mm, 0.13 – 0.17 mm thickness; Thermo Fisher Scientific, USA) using a paintbrush. The desired position (e.g., dorsal side down) was achieved by gently rolling the larva with a paintbrush.

We restored the capacity for normal movement through the delivery of water with a moistened paintbrush that had most of the bristles removed. The paintbrush was brought to the interface of the coverslip and the larval midpoint, which allowed larval hydration while preventing unwanted movement due to water adhesion and surface tension. The time from larval drying to water delivery was kept to a minimum (in all cases < 30 s) to avoid larval desiccation. This technique was often used as an alternative to the standard self-righting assay which involves rolling a larva directly on agar, and we refer to it in other sections as the ‘water unlocking technique’.

Contact based assays

The effect of localised substrate contact was tested by placing foraging third instar *w¹¹¹⁸* larvae onto a substrate with specific portions of the body touching the surface. In the dorsal contact experiments, we positioned larvae on a coverslip such that only the dorsal side contacted the surface. This involved one of three positions: the anterior half, posterior half, or whole dorsal side touching the surface. These conditions were chosen in a randomised order for each larva. After positioning, larvae were released using the water unlocking technique and we measured the occurrence and timing of self-righting within the subsequent 60 s.

For the ventral contact experiments, larvae were placed ventral side down on a coverslip, with the anterior half, posterior half or whole ventral side in contact with the surface. The larva on the coverslip was then placed dorsal side down onto a 1% agar plate, such that the whole dorsal side contacted the agar. This provided sufficient moisture to facilitate movement. We used a 3D-printed coverslip holder of 0.5 mm height to provide consistent contact to the dorsal and ventral sides of the larva. After placement, we noted the occurrence of the first behaviour. If the larva performed enough peristaltic waves to elicit a translation of more than one segment, the behaviour was labelled as crawling, even if the larva later performed self-righting.

Thermogenetic inhibition of sensory neurons

To conditionally inhibit sensory neuron populations, we used *shibire^[ts]* (*shi^[ts]*), a temperature-sensitive allele of the shibire protein which is required for synaptic vesicle recycling. Exposure of *shibire^[ts]* to restrictive temperatures above 30 °C results in synaptic vesicle depletion and cessation of synaptic transmission. We generated *shibire^[ts]* heterozygote larvae by crossing male flies carrying *UAS-shi^[ts]* with virgin females carrying a sensory domain Gal4. We collected six first instar larvae at a time and allowed them to acclimate on 1% agar at 25 °C for 5 min. We tested self-righting in the typical fashion by rolling each larva onto its dorsal side with a small paintbrush and measuring the time to the restoration of typical posture, up to a maximum of 300 s. We then transferred the agar onto a Peltier device (TC-36-25, TE Technology Inc, USA) pre-heated to 32 °C and left the larvae for 20-30 min for *shibire^[ts]* inhibition to occur. We tested self-righting again as above, before removing the agar from the Peltier, allowing a recovery of 45 – 60 min, and testing self-righting a final time. Prior to each self-righting test, larvae were gently rolled a few times, with the aim of depleting any remaining synaptic vesicles during the *shibire* inhibition. We tested control larvae homozygous for *UAS-shi^[ts]* in an identical fashion. While we started with equal sample sizes for controls, some larvae were discarded during the experiment due to wandering onto the Peltier device, leading to some small imbalances in sample sizes between the groups.

Localised optogenetic inhibition of sensory neurons (Opto-axial approach)

To locally inhibit groups of sensory neurons, we developed an optogenetic approach using physical masking of light to sets of segments along the anterior-posterior axis. We generated heterozygote larvae expressing GtACR2 in multidendritic sensory neurons by crossing male flies carrying *UAS-GtACR2* with virgin females carrying *109(2)80-Gal4* or *ppk-Gal4*. Crosses were carried out in food supplemented with ATR to a concentration of 5 mM. We selected foraging third instar larvae and allowed them to acclimatise on 1% agar for 5 min. To test a larva, we placed it dorsal side down on a coverslip and placed it in a custom 3D-printed arena. The arena contained a slit in the base measuring 8 x 1 mm through which light was delivered. We used a 1 W LED with a peak wavelength of 470 nm (OSCONIQ P3030, Intelligent LED Solutions, UK) to inhibit neurons expressing GtACR2. The LED was attached to the underside of the arena and delivered ~ 2.12 mWmm⁻² to three segments of the larva positioned above. The LED was activated manually after positioning the larva via a switch. After light delivery, the larva was quickly released using the water unlocking technique. The subsequent behaviour was recorded up until the completion of self-righting. Larvae were subjected to five illumination conditions in a random order, with light targeting four sets of three segments from anterior to posterior (T1-T3, A1-A3, A4-A6, A7-A9), and one control condition where the light was not activated (None). Control genotypes were generated by crossing one parental line with a line carrying the background genetics of the other line (i.e., *w* or *yw*), and were tested in an identical fashion. The expression strengths of the *109(2)80-Gal4* and *ppk-Gal4* lines were compared via crossing these to the line *w; +; 10XUAS-GCaMP6s::tdTomato*, then measuring fluorescence intensity of tdTomato in third instar progeny. The tdTomato fluorescence intensity was quantified as the mean grey value of an equal-sized ROI drawn around the daIV neuron ddaC, using the red channel of images acquired on a Leica DM6000. All larvae were imaged from the dorsal side. The mean fluorescence intensity was almost equal, suggesting equal expression strength within ddaC across the two drivers. The GCaMP signal was not measured.

Behavioural feature quantification

DeepLabCut implementation

To quantify features of self-righting behaviour, we first carried out tracking of larval body positions using the pose estimation machine learning tool DeepLabCut [version 2.2.3, Mathis et al., 2018]. Using recordings with a top-down view, we labelled four points along the anterior-posterior axis. This included the tip of the head, the tip of the tail, and two points close to the midpoint of the larva separated by one segment. Points were always labelled along the apparent midline of the larva, irrespective of its rotation with respect to the camera. For the training dataset, we labelled 100 frames extracted using k-means. Training was carried out with default settings (ResNet50) for 500,000 iterations. Analysis and video generation were also performed with default settings. Network performance was assessed by visual examination of videos, which showed accurate labelling in all cases. All videos input to DeepLabCut were manually trimmed so that the start and end coincided with the start and end of the behavioural sequence. All training and analyses were conducted on a PC running Windows 10 Home and using an NVIDIA RTX 2070 Super (NVIDIA, USA).

Feature calculation

Body coordinates retrieved using DeepLabCut were used to calculate behavioural features. All data wrangling and analysis was carried out in R [version 4.2.2., R Core Team, 2024]. Speed was calculated as the two-dimensional Euclidean distance travelled over each frame. Curvature angles were calculated using trigonometric functions on the vectors between the larval midpoints and the end points. Here, we extended the vector between the two midpoints to acquire a 'straight' vector. We used this as an approximation of where the head (tail) position would be if the larva had no curvature. In combination with vectors describing the position of the head (tail) with respect to the midpoint, curvature was calculated as:

$$\theta = \arccos \left(\frac{\vec{BA} \cdot \vec{BC}}{\|\vec{BA}\| \|\vec{BC}\|} \right)$$

Where BA is the vector from midpoint to head (tail) and BC is the vector from midpoint to the 'straight' head (tail). To calculate if curvature left- or right-handed, we first normalised all coordinates by rotating them with respect to the video frame, with the degree of rotation applied to align the two midpoints along the video y-axis. Left and right positions were then designated on the basis of x-axis values of the head (tail) with respect to the midpoint, with lower x values representing right-handed curvature and greater x values representing left-handed curvature. Changes in curvature direction were then calculated as the number of times the x-axis value of the head (tail) went from increasing to decreasing or vice versa.

Immunohistochemistry

Immunohistochemistry of 109(2)80>GFP embryos was carried out as previously described [Klann et al., 2021]. Embryos were collected at around 15 hours after egg laying, corresponding to developmental stage 16, to ensure sufficient development of the PNS. Dechorionation was carried out in 100% bleach for 2 min and samples were fixed for 30 min in a solution of 10% formaldehyde and heptane at a 1:1 ratio. Following an overnight incubation in methanol, embryos were rehydrated with 50% v/v methanol and PBS supplemented with 0.3% v/v Triton-X (henceforth PTBX). Embryos were then incubated with the primary antibody solution overnight at 4 °C. After washing in PBTx, the secondary antibody incubation was carried out for 2 hours at room temperature. For concentrations of primary and secondary antibodies, see Table 2.

For imaging, embryos were then mounted on a microscope slide in a solution of 75% v/v glycerol in PBS. Imaging was carried out on a Leica SP8 scanning confocal microscope. Laser power, scanning routine, aperture size, sensor gain and offset, and z-slice step size were varied depending on the sample to achieve optimal brightness, contrast and resolution in each channel. Image manipulation was carried out in FIJI, which involved image rotation, further adjustment of channel brightness and contrast, and z-projection generation.

Cell sorting and RT-PCR

Collection of multidendritic neurons from 109(2)80>GFP larvae was performed as previously described [Klann et al., 2021], following a protocol described by Harzer and colleagues for the collection of neuroblasts [Harzer et al., 2013]. Briefly, this involved the opening of newly hatched first instar larvae at different points along the body axis, before tissue dissociation using collagenase I and papain. Following washing with Rinaldini's solution and Schneider's medium, the cells were homogenised and taken for fluorescence-activated cell sorting (FACS) on a BD FACS Melody (BD Biosciences). GFP-expressing cells were collected directly into TRIzol and homogenised via vortexing, and non-fluorescent cells were discarded. Around 50 larvae were processed per replicate resulting in the collection of around 5,000 cells.

Cells collected via FACS were immediately used for RNA extraction following a standard phenol-chloroform extraction from TRIzol. Phase-separated RNA was precipitated in isopropanol and glycogen before being resuspended in RNase-free water. RNA was reverse transcribed to cDNA using the SuperScript IV kit (Invitrogen) using oligo dT(20) primers. cDNA was then amplified via polymerase chain reaction (PCR) using standard Taq DNA polymerase (NEB) for 40 cycles and with annealing temperature of 60 °C. Primers were included at a final concentration of 0.4 μM for the Hox genes antennapedia, ultrabithorax, abdominal-A and abdominal-B, as well as for the housekeeping gene rp49, the sequences of which can be found in Table 2. Following amplification, gel electrophoresis was carried out on a 2% agarose gel containing ethidium bromide and submerged in TAE buffer. The amplified DNA was run alongside a 100 bp ladder (NEB). Control samples were also run which either did not undergo reverse transcription (no RT), or lacked the cDNA in the PCR step (no template), to account for genomic DNA or non-specific amplification respectively.

Table 2. Antibodies used in immunohistochemistry.

All solutions were prepared in PBS supplemented with 0.3% v/v Triton-X.

Antibody	Type	Host animal	Source	Dilution
anti-GFP (ab13970)	Primary	Chicken	Abcam	1:100
22C10 (anti-Futsch)	Primary	Mouse	DHSB	1:10
anti-Antp 4C3	Primary	Mouse	DHSB	1:100
anti-Abd-B 1A2E9	Primary	Mouse	DHSB	1:100
Alexa-Fluor anti-chicken A488	Secondary	Goat	Invitrogen	1:500
Alexa-Fluor anti-mouse A555	Secondary	Donkey	Invitrogen	1:500

Table 3. Sequences of primers used in RT-PCR.

Gene	Forward primer	Reverse primer
<i>rp49</i>	ccgctcaaggacagtac	gcaatctccttgcgctct
<i>Antp</i>	acggagtctaccactaaa	gatctgaggtcacatgagttg
<i>Ubx</i>	gcagcgcaatgaactcgtac	tcagatggtggttgccata
<i>abd-a</i>	tccttccagatctccagtg	gtaggcctttcaatcgatgc
<i>Abd-b</i>	gctagtccagcgattggaag	gtcggttggtcacacatcag

Statistical analysis

All statistical analysis was carried out in R (version 4.2.2). Continuous response data were first checked for normality through visual examination of distributions as well as with the Shapiro-Wilk test. In the case of non-normal data, paired comparisons between experimental conditions were conducted using the Wilcoxon signed rank test. Relationships between continuous data (and count data) were assessed with Spearman correlations.

For continuous data predicted by multiple factors, such as self-righting times under localised optogenetic inhibition, we fit linear mixed effects models. Data were log-transformed to improve model fit. If a given predictor had a single control level (illumination condition), we used treatment contrasts; otherwise, effects contrasts were used (genotype). Fixed effects were estimated for experimental manipulations (genotype, illumination condition) while random intercepts were estimated to account for sample effects. Model fit was assessed by visual examination of residual and random effect distributions as well as numerical examination with the Shapiro-Wilk test; model fit was ideal in all cases. P-values for marginal model effects were calculated following analysis of deviance with F-tests. In the case of a significant interaction effect, we conducted post-hoc contrasts of estimated marginal group means, conditional on genotype. To reduce the number of post-hoc tests, we followed Dunnett's approach to compare each experimental condition with the control condition. One-sided tests were used in the case of a specific hypothesis of response increase or decrease. P-values were adjusted with Sidak's correction for multiple comparisons.

Count data predicted by multiple factors, such as the number of head casts during self-righting, were modelled in a similar fashion as above but using negative binomial models. Model fit was assessed by calculating the ratio of residual deviance to degrees of freedom of the residuals. P-values for marginal model effects were calculated following analysis of deviance with χ^2 tests. Post-hoc comparisons were carried out as described above for continuous data.

Matched binary data, such as the occurrence of self-righting under localised substrate contact, were tested with Cochran's Q test. The test was first applied across conditions to infer the existence of group differences, before being applied pairwise between groups (where it is equivalent to the McNemar test) to determine the location of the significant differences.

Results

Self-righting behaviour involves greater speed and curvature of the head than tail

A simple visual characterisation of self-righting behaviour (as has been done previously, see [Picao-Osorio et al., 2015](#)) suggests that the sequence involves differential movement of body regions along the anterior-posterior axis over time [[Figure 1A](#)], an observation that has been supported quantitatively by a study employing physical modelling of larval movement [[Loveless et al., 2021](#)]. Furthermore, observation of this behaviour in a variety of model animals – across which it is highly conserved, including in humans [[Figure 1B](#)] – also points to a particular involvement of the anterior region of the body in initiating the first stages of rotation that is key to the proper execution of the sequence. However, it remained unclear how these regional differences might relate to the specific sensory conditions that induce self-righting. To ratify previous findings, and establish a framework for further behavioural analyses, we sought to develop a quantitative account of typical self-righting behaviour. To this end, we established a novel method for controlling larval posture we call the 'water-unlocking technique', which enabled us to record self-righting behaviour in a controlled and reproducible manner. This method involved the positioning of a third-instar w^{1118} larva in the dorsal-down posture on a dry glass surface. The induction of self-righting was then elicited by the delivery of a water droplet, which permitted the larva to move freely while behaviour was recorded [[Figure 1C](#)]. To generate data on the posture of larvae throughout self-righting, we analysed recordings with DeepLabCut, a deep learning

algorithm to track body coordinates over time [Mathis et al., 2018]. We labelled four points along the AP axis – head, tail and two middle points – from which we calculated speed and curvature angle of the head and tail [Figure 1D].

When examining head and tail speed over the course of entire recordings, we noticed a similar trend for both body parts, involving an initial lull of activity that increased towards the end of the recording [Figure 1E, F]. Since we wanted to focus on the self-righting sequence itself, we subset the data based on head movement to exclude the initial lull phase [green bar, Figure 1E]. As expected, we observed that speed during the self-righting sequence was significantly greater for the head than for the tail [Figure 1G], confirming the notion that the anterior plays an important role. Since lateral bending of the body is also a key part of the self-righting sequence [Picao-Osorio et al., 2015] we also examined the trends of absolute curvature of the head and tail over time. Interestingly, the average curvature for the head appeared to follow three distinct phases, characterised by a relatively steady degree of curvature that quite suddenly increased to a higher degree of steady curvature [Figure 1H, purple]. We suggest this observation likely reflects a repeated back-and-forth bending of the head that occurs prior to the rotational aspect of self-righting, which only occurs after opportunities for surface attachment have been exhausted. In contrast, the tail showed no such changes in curvature, with the curvature angle only subtly increasing in magnitude over the course of the behaviour [Figure 1H, red]. To better understand the distribution of curvature angles, as well as their directionality, we examined the probability densities for relative head and tail angles. For the tail, angles were somewhat normally distributed around zero, albeit with a small hump at 30° to the left [Figure 1I, red], suggesting that most tail angles are quite small, although there may be a slight preference for left-handed bends. Oppositely, the distribution for head angles was centred slightly left of zero, and showed distinct peaks at around 50° to both the left and the right [Figure 1I, purple]. This indicates that while head curvature is stronger than that of the tail, it tends to more often occupy a specific range of moderate curvature at around 50°. While these angle distributions suggested a possible chirality in the curvature occurring during self-righting, which showed a slight group-level preference for left-handed bends [Supplementary material Figure S1]. Direct comparison of the absolute curvature angles confirmed that head angles were indeed significantly greater than tail angles [Figure 1], indicating that self-righting involves a particularly strong bending of the head. Overall, these results indicate that unlike other behaviours such as rolling [Cooney et al., 2023], self-righting is characterised primarily by movement and bending of the head, which tends to follow a profile of increased but moderate bending over time.

Larval self-righting requires anterior dorsal contact but is abolished by ventral anterior contact

Our initial analysis of self-righting behaviour revealed a clear preference for anterior movement and curvature over that of the posterior. Because different behavioural sequences are often related to the presence of specific sensory stimuli, we questioned to what extent this asymmetry in muscle contractions was related to spatial differences in sensory processing. While it was apparent that self-righting depends on substrate contact at the dorsal side of the body, and not gravity [Klann et al., 2021], it was unknown if sensory stimuli at different areas along the AP axis would result in different behavioural outcomes. To tackle this problem, we devised a set of experiments involving the presence of substrate contact at restricted regions along the AP axis. We again used the water-unlocking technique in order to precisely position larvae in the desired posture [Figure 2A]. We placed each third instar *w¹¹¹⁸* larva in three positions with dorsal substrate contact: whole body contact, the anterior half only, or the posterior half only [Figure 2B], and observed the occurrence of self-righting. As expected, whole body contact led to the performance of self-righting as usual. Interestingly, while the majority of larvae also performed self-righting in the anterior contact position, the posterior contact condition failed to elicit self-righting in most larvae [Figure 2C], suggesting anterior substrate contact is required for self-righting. While we observed no clear visual differences self-righting sequence between the whole body and anterior only conditions, comparison of self-righting times suggested a slight trend

towards faster times in the anterior-only condition [Figure 2D]. We suspect this is due to reduced friction experienced by larvae in the anterior contact condition, allowing them to complete the behaviour slightly faster than with whole body substrate contact.

Given the apparent role of localised dorsal contact in eliciting self-righting, we then questioned if self-righting can still occur under a combination of dorsal and ventral substrate contact. Specifically, we were primarily interested to test if any differences would be observed with ventral contact present at different regions along the AP axis. To test this, we arranged larvae ventral side down on the substrate. We then subsequently placed the larvae dorsal side down onto an agar substrate, providing whole body dorsal contact and permitting movement from the moisture of the agar. We used a 3D-printed spacer to provide consistent contact to the two sides of the larva [Figure 2E]. As with the dorsal contact experiments, we placed larvae in three positions of ventral contact: whole body, anterior half, or posterior half only [Figure 2F]. Across these conditions, we observed an inverse effect to that of the localised dorsal contact: while the posterior only ventral contact permitted self-righting in most cases, both whole body and anterior-only ventral contact largely prevented the occurrence of the behaviour [Figure 2G]. These latter conditions instead elicited crawling in the majority of larvae, suggesting that anterior ventral contact is sufficient to suppress self-righting in favour of crawling despite the continued presence of dorsal substrate contact. In combination, these results highlight the anterior of the larva as a key region for the modulation of behaviour through mechanosensory stimulation.

Conditional inhibition of multidendritic neurons delays self-righting

Although our results thus far suggested that self-righting depends on mechanical stimulation at the anterior, it remained unknown how this stimulation was received by mechanosensory neurons. Therefore, we decided to explore how self-righting behaviour correlated with the activity of localised mechanosensory neurons. However, it also remained unclear what populations of sensory neuron types were responsible for detecting substrate contact. While previous research suggested a role of the multidendritic neurons – in particular the highly branched daIV neurons – this relied on constitutive inhibition of these cells throughout development [Klann et al., 2021], which could have produced off-target knock-on effects on the rest of the nervous system [Fushiki et al., 2013; Kaneko et al., 2017]. Thus, we wished to implement a conditional approach to temporarily inhibit various groups of sensory neurons, which display a stereotyped arrangement along the AP axis [Figure 3A]. To achieve this, we used the Gal4/UAS system to express a temperature-sensitive allele of *shibire* (*shi^{ts}*) in subpopulations of sensory neurons, which impairs synaptic transmission when exposed to temperatures greater than 30 °C [Kitamoto, 2001; Kasuya et al., 2009]. We tested self-righting behaviour under synaptic inhibition by measuring the time taken by first instar larvae to right themselves on an agar substrate after being rolled over with a paintbrush. To control for the effects of *shi^{ts}* at the restrictive temperature of 32 °C, we also assayed self-righting before and after this inhibition at a permissive temperature of 25 °C [Figure 3B].

Given the previous finding of a contribution of multidendritic (md) neurons to self-righting, we first tested inhibition in the 109(2)80-Gal4 domain, which drives expression in all multidendritic neurons [Gao et al., 1999] as well as in some oenocytes and chordotonal organs [Grueber et al., 2002], and also a few cells in the CNS [Hughes & Thomas, 2007]. Because md neurons in general comprise several classes of sensory neurons, their testing emerged as a suitable starting point for our conditional inhibition analysis.

Our results show a significant increase in self-righting times at the restrictive temperature, confirming the suggestion that multidendritic neurons play a role in self-righting. However, the entire set of multidendritic neurons contains several classes of neurons that detect both external mechanical stimuli (daII, daIII and daIV) [Hwang et al., 2007; Tsubochi et al., 2012; Yan et al., 2013] as well as proprioceptive feedback (daI, bd) [Hughes & Thomas, 2003; Vaadia et al., 2019]. To narrow down the multidendritic population, we also tested other Gal4 lines with class-specific expression domains. We initially reasoned that since substrate contact is an innocuous

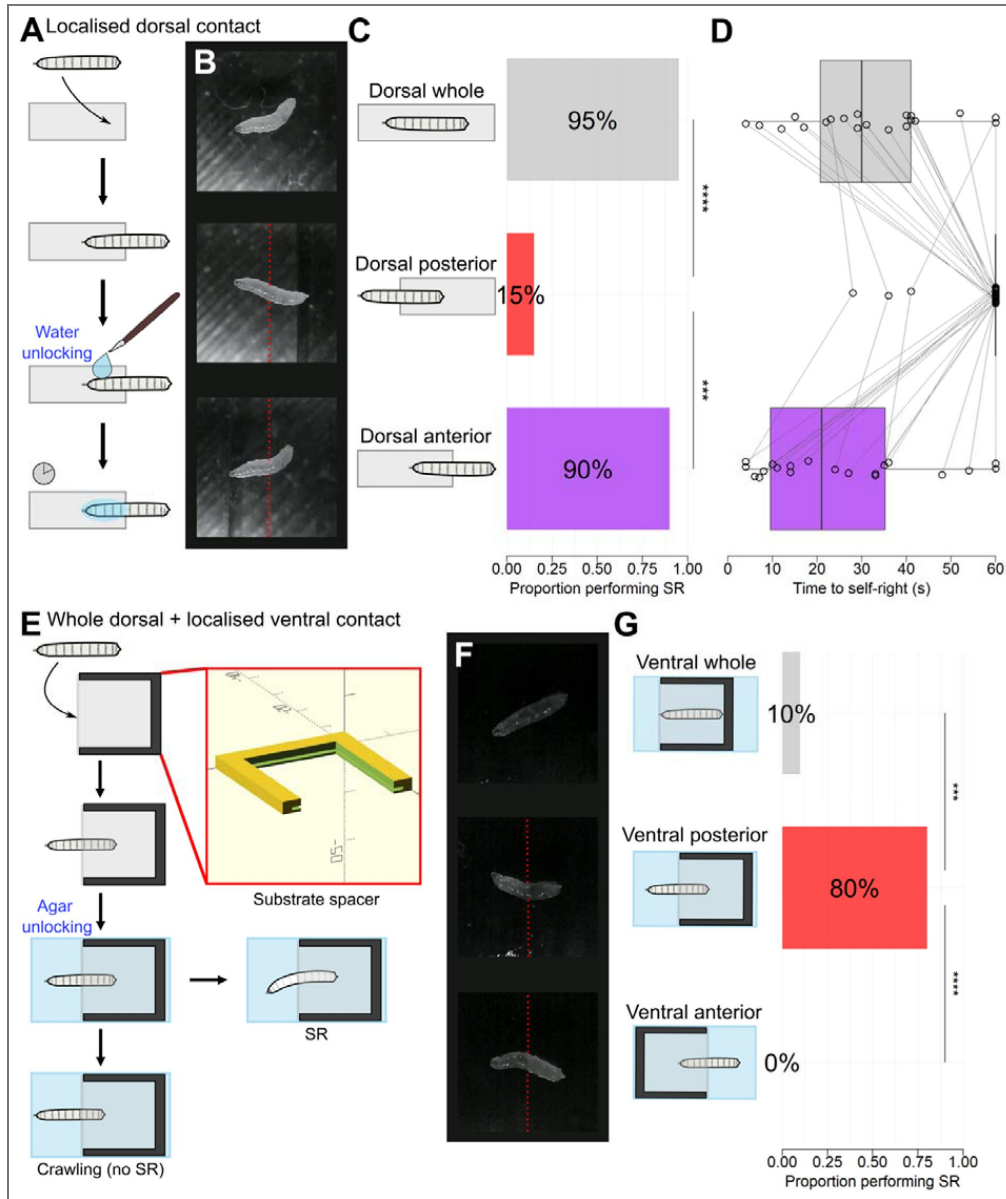


Figure 2. Effects of localised substrate contact on self-righting.

A) Experimental procedure for investigating localised dorsal substrate contact. Third instar w^{1118} larvae were first placed dorsal side down on a dry glass coverslip in the desired position. Movement was then unlocked via the application of water with a paintbrush. **B)** Photographs of larvae in three conditions of dorsal substrate contact. The red dashed line indicates the boundary of the coverslip. **C)** Proportion of larvae that performed self-righting in the three conditions of dorsal substrate contact. Group comparison: Cochran's $Q_{(2)} = 28.35$, $P < .001$, $n = 20$. '****' = $P < .001$, '***' = $P < .01$ for pairwise Cochran Q tests. **D)** Self-righting times in the three conditions of dorsal substrate contact. For larvae that didn't self-right within 60s, the time is shown as 60. Points show times for individual tests, with measurements from the same larva being connected by lines. The box and whisker plots indicate the median, IQR and 1.5 IQR. $P = 0.047$ for a Wilcoxon signed rank test comparing the anterior and whole-body conditions, $n = 17$. **E)** Experimental procedure for investigating the combination of whole-body dorsal substrate contact with localised ventral substrate contact. A coverslip was held inside a custom 3D-printed mount (red box) to provide consistent contact. Third instar larvae were placed ventral side down on the coverslip in the desired position. The coverslip and larva were then placed onto agar, providing whole-body dorsal contact and sufficient moisture for movement. Larvae generally performed crawling or self-righting. **F)** Snapshots of larvae in the three conditions of ventral substrate contact. The red dashed line indicates the boundary of the coverslip. **G)** Proportion of larvae that performed self-righting in the three conditions of ventral substrate contact. Group comparison: Cochran's $Q_{(2)} = 29.50$, $P < .001$, $n = 20$. '*****' = $P < .0001$, '****' = $P < .001$ for pairwise Cochran Q tests. The mean self-righting time for larvae that performed self-righting with ventral contact was 32.8 seconds.

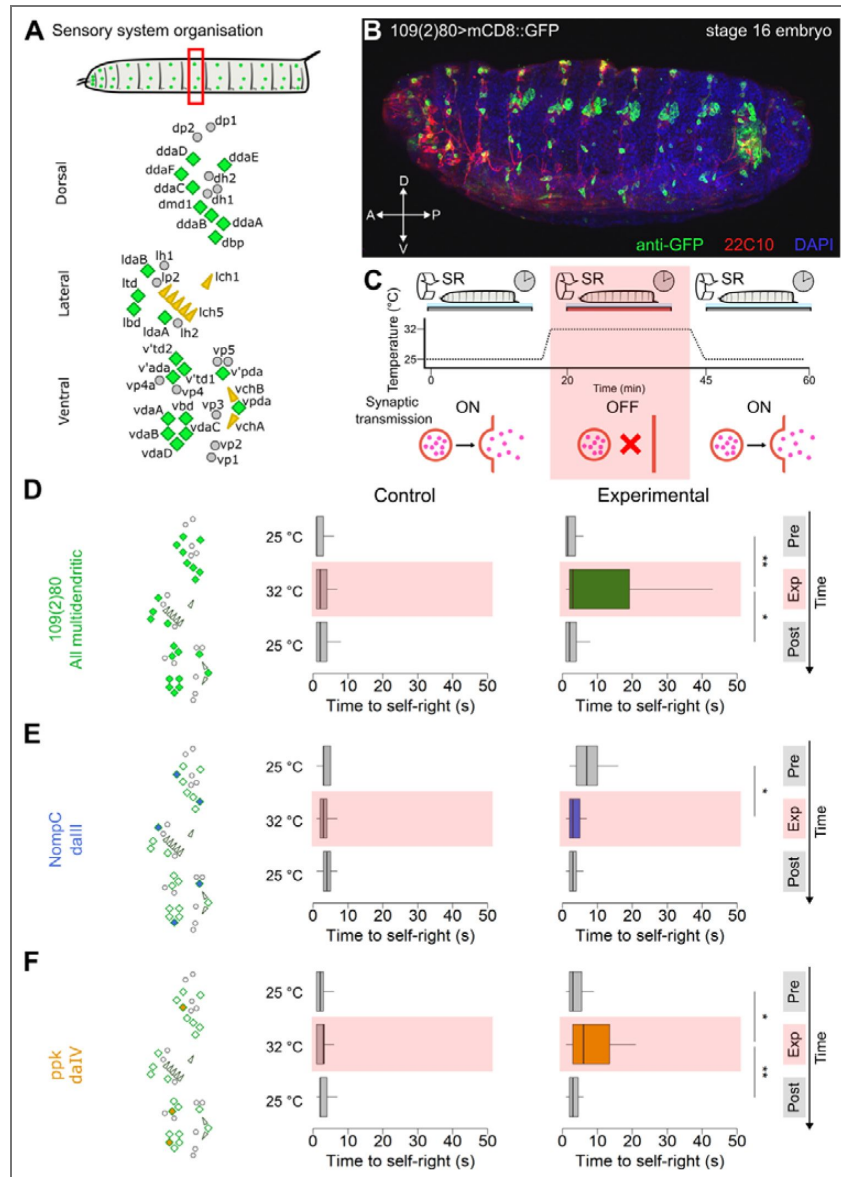


Figure 3. Conditional thermogenetic inhibition of multidendritic sensory neurons

A) The peripheral nervous system of the *Drosophila* larva. The diagram (top) shows the larva with the segmentally repeated clusters of sensory organs. The canonical hemisegmental arrangement (bottom) shows the es organs (grey circles), chordotonal organs (yellow triangles) and multidendritic neurons (green diamonds). Adapted from Orgogozo & Grueber (2005). **B)** A confocal z projection of a stage 16 embryo with GFP expression in the 109(2)80-Gal4 domain. The embryo has been immunolabelled with anti-GFP (green), 22C10 (axonal tracts, red) and DAPI (nuclei, blue). **C)** Experimental procedure for conditional inhibition of sensory neurons expressing *shibire*^[ts] (*shibire*^[ts]). Self-righting is first performed with first instar larvae at 25 °C, at which *shibire* is functional and synaptic transmission occurs normally. The substrate is then heated to 32 °C and self-righting is tested again. This temperature impairs *shibire* function and inhibits synaptic vesicle recycling and release. The temperature is then lowered back to 25 °C allowing restoration of *shibire* function. Self-righting is tested again to ensure recovery from the conditional inhibition. **D-F)** Self-righting times for first-instar larvae expressing *shibire* in different sets of sensory neurons. In each case, the location of the sensory neuron population within the hemisegmental arrangement is shown (left). Box and whisker plots indicate self-righting times in each temperature condition, for *UAS-shibire*^[ts] controls (left) and age-matched experimental genotypes (right). The temporal order of the temperature conditions follows from top to bottom of each plot. * = $P < .05$, ** = $P < .01$, *** = $P < .001$ for pairwise Wilcoxon signed-rank tests. Individual observations are not displayed for visualisation purposes due to large variance. **C)** Self-righting times of *109(2)80>shibire*^[ts] larvae, expressing *shibire*^[ts] in all multidendritic neurons. $n_{[exp]} = 38$, $n_{[control]} = 37$. **D)** Self-righting times of *NompC>shibire*^[ts] larvae, expressing *shibire*^[ts] in daIII neurons. $n_{[exp]} = 17$, $n_{[control]} = 17$. **E)** Self-righting times of *ppk>UAS-shibire*^[ts] larvae, expressing *shibire*^[ts] in daIV neurons. $n_{[exp]} = 39$, $n_{[control]} = 40$.

mechanical stimulus, it might depend on the daIII neurons, which are known to respond to gentle touch [Yan et al., 2013]. Thus, we tested the conditional inhibition in the NompC-Gal4 domain, which drives expression in the daIII neurons. Contrary to our hypothesis, self-righting was not delayed at the restrictive temperature; in fact, there was a trend towards faster self-righting times at this temperature [Figure 3D], suggesting that daIII neurons are not vital for detecting the substrate contact that induces self-righting. An alternative population of sensory neurons is the highly branched daIV neurons. This population have been strongly implicated in nociception due to their involvement in rolling behaviour [Tracey et al., 2003; Hwang et al., 2007; Ohyama et al., 2013]; however, they have also been linked to sensory feedback during crawling behaviour [Ainsley et al., 2003; Gorczyca et al., 2014; Jang et al., 2019], as well as to self-righting [Klann et al., 2021]. In agreement with previous findings, we indeed found that inhibition of daIV neurons via the ppk-Gal4 domain caused substantial delays in self-righting times [Figure 3E], suggesting that these neurons are indeed important for normal self-righting behaviour. However, the effect size was smaller than that for the entire multidendritic population, suggesting neurons other than the daIVs are important for self-righting. Since they have been implicated in other behaviours like rolling and crawling [Caldwell et al., 2003; Ohyama et al., 2015], we also examined the effect of chordotonal organ (CO) inhibition on self-righting. While we did observe a strong effect on self-righting times [Supplementary material Figure S2], we did not pursue this further: given the anatomical distributions of CO in lateral and ventral-only locations, it is hard to conceive a way in which they could detect dorsal-only contact over ventral-only [Hartenstein, 1988]; also, their known functions as proprioceptors [Caldwell et al., 2003] likely preclude a role in regional substrate detection.

In all cases, we observed little effect of temperature on larvae expressing *UAS-shi^{ts}* in the absence of Gal4. Although there were some trends for shorter self-righting times at the restrictive temperature, this is in line with the known effects of temperature on other behaviours like crawling [Evans et al., 2023]. Overall, through conditional inhibition, these results demonstrate the importance of the proper function of multidendritic neurons for the triggering of an effective self-righting behaviour.

Optogenetic inhibition of anterior but not posterior multidendritic neurons delays self-righting

Having observed that normal activity of multidendritic sensory neurons was important for self-righting, we wished to reconcile this finding with the previous observation of an anterior dominance in self-righting. Specifically, we aimed to determine if the anterior multidendritic neurons were responsible for registering the sensory inputs required to induce self-righting. To this end, we developed a novel approach to achieve spatially-restricted neuronal inhibition in a freely moving larva, a technique that we coined the “opto-axial method”. We designed a custom 3D-printed arena containing a small slit, which acts as a photomask for an LED positioned underneath [Figure 4A]. This approach allowed us to target three segments on a third-instar larva, which we accurately positioned and recorded using the water-unlocking technique [Figure 4B]. To test the effect of neuronal location on self-righting, we placed each larva in five positions: four positions which targeted segments along the AP axis and one control position with no light [Figure 4C], following a randomised order. We elicited optogenetic inhibition of multidendritic neurons via expression of the photosensitive anion channel GtACR2 [Govnorova et al., 2014] in the 109(2)80-Gal4 domain.

Mirroring our results with substrate contact, we found that inhibition of multidendritic neurons in the anterior regions comprising segments T1-T3 and A1-A3 significantly prolonged self-righting compared to the no illumination condition. Conversely, inhibition in the more posterior regions comprising segments A4-A6 and A7-A9 had little effect on self-righting times [Figure 4D], suggesting that anterior multidendritic neurons are uniquely responsible for directing self-righting behaviour. Furthermore, the effect size of inhibition on self-righting time was similar for segments T1-T3 and A1-A3, indicating the existence of a relatively sharp transition in self-righting-relevant activity at around halfway along the AP axis, as opposed to a sensory gradient from

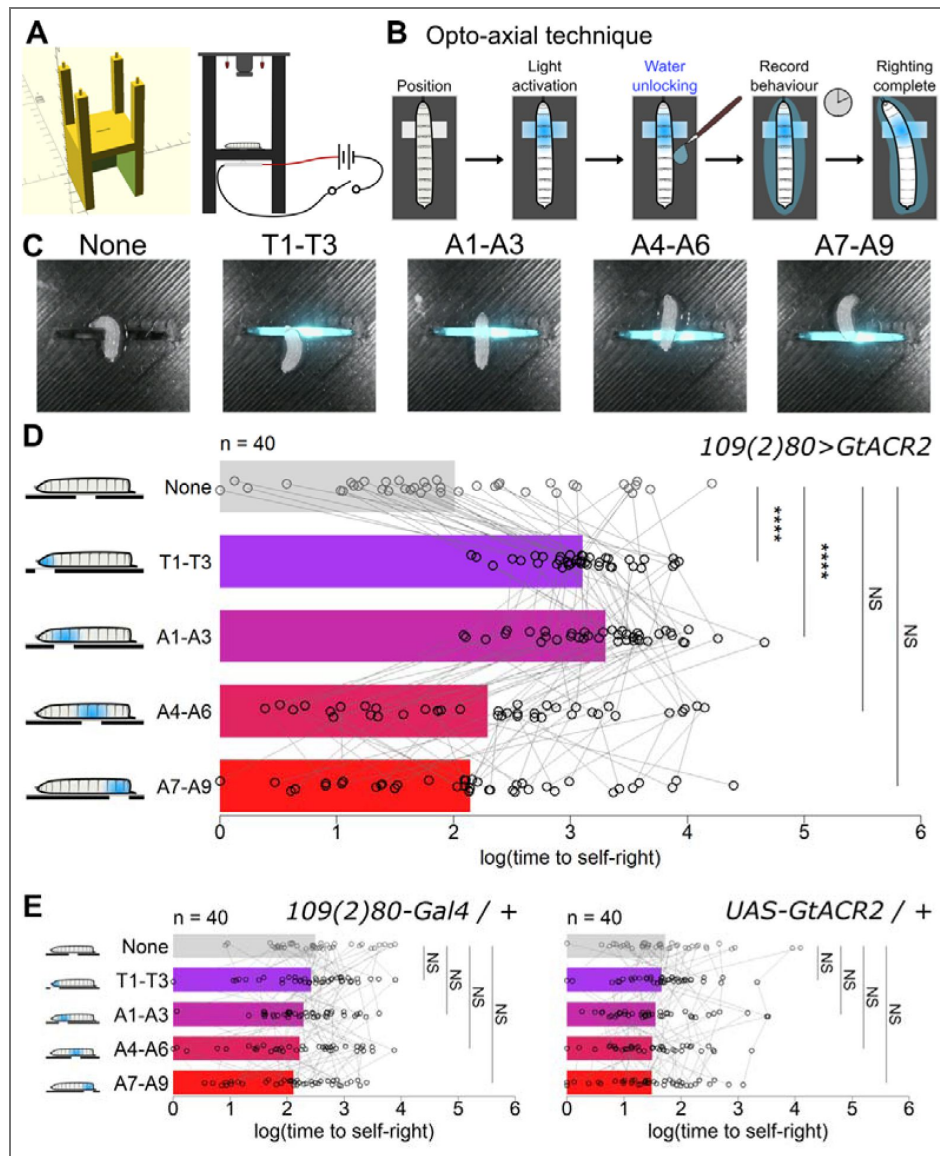


Figure 4. Localised optogenetic inhibition of multidendritic sensory neurons along the anterior-posterior axis.

A) Experimental setup for localised optogenetic inhibition. Inhibitory light was spatially restricted by means of a small slit in the base of a 3D-printed arena (left). The LED was positioned under the slit and operated by a switch, while an infrared camera recorded from above (right). **B)** Experimental procedure for testing the effects of localised inhibition on self-righting. Larvae were positioned dorsal side down on a coverslip above the slit such that incoming light illuminated a group of three segments. After light activation, larvae were quickly unlocked through application of water and the time to complete self-righting was timed. **C)** Photographs of the five experimental conditions of localised illumination. In each condition, light targeted a group of three segments along the anterior-posterior axis, while no light was used as a control condition. **D)** Log-transformed time to self-right across the five illumination conditions for larvae expressing GtACR2 in the 109(2)80 domain. The bars show mean values, and points show individual measurements with measurements from the same larva being joined by grey lines. Analysis of deviance for a mixed model including control genotypes revealed a significant interaction of illumination condition and genotype ($F_{(8, 468)} = 10.35, P < .001, n = 40$). '****' = $P < .0001$, NS = $P > .05$ for post-hoc one-sided comparisons between conditions of light illumination, following Dunnett's approach with Sidak's adjustment for multiple comparisons. **E)** Log-transformed time to self-right across the five illumination conditions for Gal4 (left) and UAS (right) genetic control lines. No statistical differences were observed between the control condition and the experimental illumination conditions for either control line.

posterior to anterior. We observed no differences in self-righting times between conditions of regional illumination in genetic control larvae that were subjected an identical experimental procedure [Figure 4E] showing this effect was indeed due to neuronal inhibition rather than light illumination alone. Visual inspection of recordings showed that while the no light and posterior conditions produced a relatively normal self-righting sequence in experimental larvae, the anterior inhibition appeared to lead to a more disorganised movement sequence with tight muscle contractions as has been reported previously for multidendritic inhibition [Hughes & Thomas, 2007]. In conclusion, these results demonstrate that specific activity of the anterior multidendritic neurons is key to effective and coordinated self-righting behaviour.

Given the current results of thermogenetic inhibition and those from prior studies showing a role of the daIV subpopulation in self-righting [Klann et al., 2021], we elected to repeat the opto-axial approach using the *ppk-Gal4* driver, which drives expression solely in daIV md neurons. We observed the same pattern as with the 109(2)80-Gal4 domain, with inhibition of daIVs in T1-T3 and A1-A3 regions leading to significantly longer self-righting times compared to no illumination, while inhibition in A4-A6 and A7-A9 had no effect. No changes in self-righting times according to illumination condition were observed in genetic control lines [Figure S3]. However, as with thermogenetic inhibition, the effect size of the self-righting delay was reduced compared to the 109(2)80-Gal4 domain. One possible explanation for this consistent difference in effect size is the relative expression strengths of the two Gal4 drivers. However, measurements of tdTomato fluorescence expressed in daIV neurons via the two drivers indicated no difference in expression level [Figure S3 C]. This suggests that suggesting that md neurons other than daIVs play a role in facilitating the efficient completion of self-righting behaviour. Given that daIII neurons appeared not to contribute to normal self-righting, the daI or daII neurons could be involved, whose contribution may be more proprioceptive in nature.

Inhibition of anterior multidendritic neurons is associated with increased head casting during self-righting

Although inhibition of anterior multidendritic neurons led to impaired self-righting behaviour, we were still unsure as to what role these localised neurons played in shaping the self-righting sequence. While visual examination of larval behaviour suggested that anterior sensory inhibition produced a more disorganised self-righting sequence, we questioned exactly how the self-righting sequence was changed. In other words, we wished to extract the precise features of movement that were altered under anterior inhibition using our framework for self-righting quantification first detailed in Figure 1. To obtain this quantification, we trained a separate network through DeepLabCut using recordings of larvae undergoing optogenetic inhibition that were trimmed to include only the behavioural sequence [Figure 5A]. As before, we achieved accurate tracking of four points along the AP axis that labelled the head, tail and two middle points.

As our initial characterisation of self-righting behaviour revealed the importance differences between mean head and tail speeds, we again analysed this feature in larvae that underwent the regional optogenetic inhibition. For head speed, we observed a reduction in mean speed for experimental larvae, but only in the A1-A3 condition. Conversely, for tail speed, we observed reductions in both the T1-T3 and A1-A3 conditions [Supplementary material Figure S4]. However, from this result alone it was still not entirely clear whether decreased speed was in fact related to increased self-righting times. To test the relationship between the two features, we calculated the spearman correlations between counts of mean head and tail speeds and self-righting times. For head speed, there was a moderate negative correlation with self-righting time for the 109(2)80>GtACR2 larvae across all illumination conditions ($\rho = -.60$, $P < .001$). Similarly for tail speed, there was a large negative correlation with self-righting time in the same conditions ($\rho = -.73$, $P < .001$). However, when we constrained the analysis to just the T1-T3 and A1-A3 conditions where self-righting time was experimentally delayed, the correlation magnitude dropped substantially for both head ($\rho = -.16$, $P = .0159$) and tail speeds ($\rho = -.30$, $P = .007$). This suggests that reductions in speed likely do not fully explain reductions in self-righting time caused by inhibition of anterior sensory neurons. Furthermore, we also observed an increase in head speed in the T1-

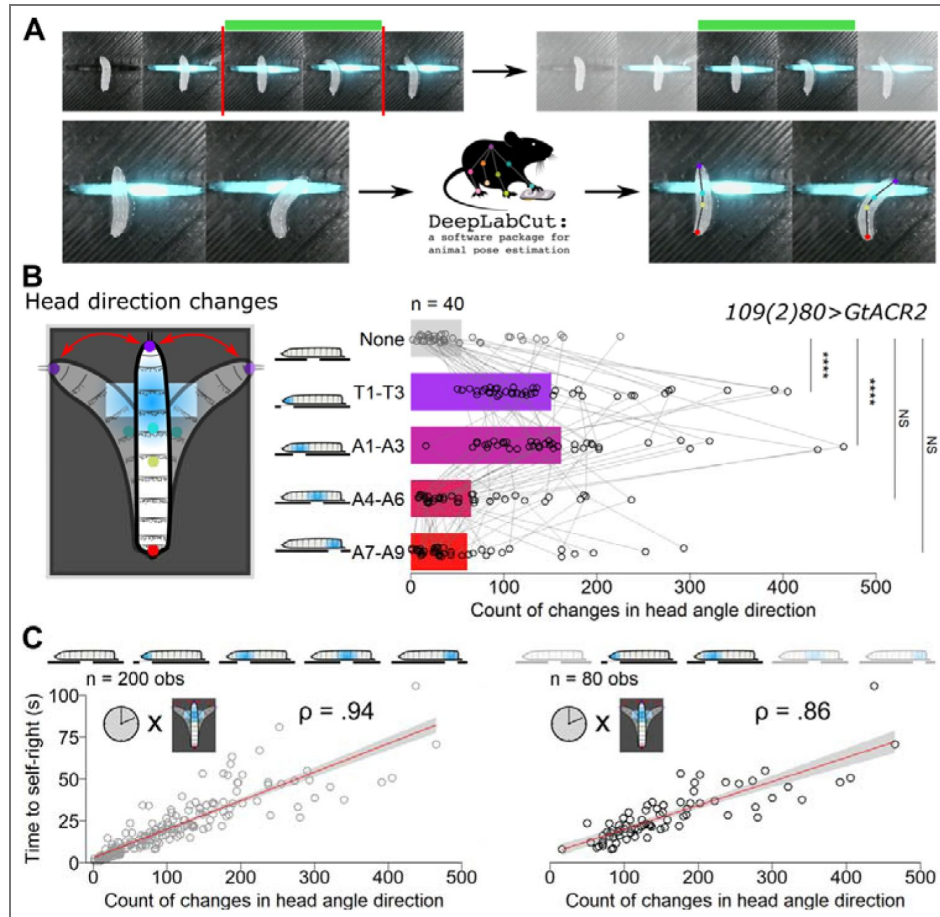


Figure 5. Behavioural changes occurring under localised optogenetic inhibition of sensory neurons

A) Labelling of recordings using DeepLabCut. Recordings of optogenetically-inhibited larvae were first manually trimmed so they contained only the time from movement unlocking to completion of self-righting (top). These videos were then analysed by DeepLabCut, which tracked four points along the anterior-posterior axis: head (purple), anterior middle (cyan), posterior middle (yellow), and tail (red). The coordinates of these tracked points were then used to calculate features of self-righting.

B) Counts of the changes in head curvature direction under localised optogenetic inhibition of multidendritic neurons. The counts were calculated as the number of times a larva went from bending towards one direction with the head to bending in the other direction. Bars show the mean values for each condition, while points show counts for individual samples with measurements from the same larva being connected by lines. Analysis of deviance for a negative binomial model including control genotypes revealed a significant interaction of illumination condition and genotype ($\chi^2_{(8)} = 40.41$, $P < .001$, $n = 40$). '****' = $P < .0001$ for post-hoc one-sided comparisons between conditions of light illumination, following Dunnett's approach with Sidak's adjustment for multiple comparisons. **C)** Correlations between count of head direction changes and self-righting times, for all illumination conditions (left) and just the anterior illumination conditions (right) in $109(2)80>GtACR2$ larvae. Points show individual observations, while the red line indicates a linear regression. $P < .0001$ for both Spearman correlations.

T3 condition for UAS-GtARCR2 control larvae [Supplementary material Figure S4 [↗](#)]. These findings led us to infer that speed was not an ideal predictor for changes in self-righting time due to sensory manipulation and prompted us to search for other factors that were more strongly associated with self-righting delays. Given the importance of head and tail bending during self-righting behaviour, we reasoned that the degree of curvature could be altered across conditions of regional illumination. However, we found no differences in mean absolute curvature across any illumination conditions for any genotypes [Supplementary material Figure S5 [↗](#)], suggesting that the ability of larvae to form bends appropriate to self-righting behaviour was not impacted by our experimental manipulation. Therefore, it appeared self-righting delays under anterior sensory inhibition were not due to larvae simply moving more slowly than normal or not achieving the optimal degree of curvature required for self-righting.

We reasoned that instead of simple changes to high-level features of larval movement, anterior sensory inhibition may be impacting the precise pattern of movements prior to self-righting completion. Another visual inspection of recordings showed that while head speed and curvature was indeed comparable to the normal sequence, the head appeared to make many more back-and-forth movements under anterior sensory inhibition, reminiscent of head casting behaviour [Ohyama et al., 2013 [↗](#)]. We sought to quantify this observation by counting the number of times that larvae changed the head angle direction; that is, going from bending towards the right to bending towards the left or vice versa. In comparing the count of head direction changes across the regions optogenetic inhibition, we observed a pattern that strikingly matched that of the self-righting times, with significantly increased counts in the anterior T1-T3 and A1-A3 conditions but not the posterior A4-A6 and A7-A9 conditions [Figure 5B [↗](#)]. We also observed no increases in counts of head curvature changes in genetic control larvae [Supplementary material Figure S6 [↗](#)]. This result confirms our observation that inhibition of anterior multidendritic neurons causes a shift to a more disorganised self-righting sequence that is characterised by a high preponderance of head casting behaviour. This finding could reflect the possibility that under anterior sensory inhibition larvae are unable to properly detect the underlying surface, and so employ a repeated head sweeping behaviour in order to find a suitable substrate for attachment.

As we did previously for movement speeds, we wanted to know if this increased head casting behaviour was relevant to increases in self-righting times. We first calculated spearman correlation coefficients for 109(2)80>GtACR2 larvae across all illumination conditions, to see if number of head casts was generally related to differences in self-righting times. Here, we found an extremely strong correlation ($\rho = .94$), showing that the natural variability in the timing of the self-righting sequence can be largely accounted for by the number of head casts. However, we also wished to see if this relationship held in the experimental conditions of anterior sensory inhibition where self-righting time was prolonged. When we restricted data to the T1-T3 and A1-A3 conditions, we observed a slightly reduced albeit very strong correlation ($\rho = .86$) between head direction changes and self-righting times [Figure 5C [↗](#)]. This supports the notion that this natural relationship still holds for experimental conditions of anterior sensory perturbation, where larvae performed much more head casting overall. In conclusion, our quantification of the features of self-righting shows that anterior sensory inhibition does not alter simple features of speed or curvature but rather causes a behavioural switch to increased head casting behaviour that well explains the delays in self-righting completion.

Since inhibition of the anterior daIVs specifically also resulted in increases in self-righting times, we questioned if an increase in head casting behaviour also occurred with this sensory subpopulation. Indeed, we observed significantly increased number of head casts in the T1-T3 and A1-A3 conditions, but not in the A4-A6 or A7-A9 conditions. As with all md neurons, this the number of head direction changes was significantly correlated with self-righting times, across both all conditions and the anterior illumination conditions only [Figure S7 [↗](#)]. This suggests that the switch to head casting behaviour over self-righting under anterior sensory inhibition is unlikely to be driven primarily by impaired proprioceptive input, but rather by an inability to

sense the underlying substrate. We speculate that increased head casting under anterior sensory inhibition likely reflects a search strategy for a suitable substrate, as the larvae are unable to detect the substrate underneath them on which they would typically self-right.

Normal expression of the *Drosophila Hox* genes *Antennapedia* and *Abdominal-B* in multidendritic neurons is required for self-righting behaviour

Our results thus far demonstrated a clear anterior precedence of self-righting behaviour, which involves not only anterior-dominated movements but also a key role of the anterior sensory system in detecting the substrate contact that elicits this postural behaviour. We thus wondered what genetic mechanisms may underlie the establishment of this pattern. Given the clear discrepancies of self-righting behaviour aligning with the AP axis, we questioned if the *Hox* genes, which play a key role in the developmental allocation of cellular identity along to this very axis, might play a role.

To first address this possibility, we first sought to determine if the sensory neurons involved in self-righting did indeed express any *Hox* genes at the larval stage. For this we used fluorescence-activated cell sorting (FACS) to collect multidendritic neurons from first instar larvae expressing GFP in the *109(2)80-Gal4* domain, extracting RNA from collected cells to carry out RT-PCR to amplify products derived from the four *Hox* genes: *Antennapedia* (*Antp*), *Ultrabithorax* (*Ubx*), *abdominal-A* (*abd-A*) and *Abdominal-B* (*Abd-B*). We selected these *Hox* genes based on their axial expression domains across other, relevant tissues (epidermis, central nervous system) of the embryonic and larval *Drosophila* [Mallo & Alonso, 2013]. Analysis of the resulting amplicons confirmed expression of all *Hox* genes tested; however, bands were particularly bright and sharp for *Antp* and *Abd-b* [Figure 6A], indicative of strong expression of *Antp* and *Abd-b* RNA in multidendritic neurons.

Having observed *Hox* expression in larval multidendritic neurons, we next questioned if a specific level of *Hox* expression was important for sensory contributions to self-righting behaviour. We hypothesised that expression of the more anterior *Hox* genes – *Antp* and *Ubx* – would influence self-righting, given the importance of anterior sensory neurons in self-righting. To test this hypothesis, we used RNAi to knockdown expression of the above noted four genes within the *109(2)80-Gal4* domain of first instar larvae, and tested self-righting times against an empty RNAi control. Intriguingly, while RNAi against *Antp* induced a substantial delay of self-righting times, no effect was observed for *Ubx*; instead, we found RNAi against *Abd-b* also produced a statistically significant, yet modest, increase in self-righting times [Figure 6B]. This latter finding may be related to the known role of posterior segments in guiding motor sequences, as has been recently observed for locomotion [Jonaitis et al., 2024]. Conversely, the former finding could be explained by *Antp* expression within anterior sensory neurons being essential for normal activity levels, as has also been demonstrated for *Hox* genes in other cellular populations [Picao-Osorio et al., 2015; Issa et al., 2019]. Given our previous results regarding daIV neurons, we also questioned if knockdown of *Hox* genes within this population also resulted in self-righting delays. Interestingly, we observed no effect of *Hox* gene knockdown within the *ppk-Gal4* domain [Figure S8], suggesting that multidendritic neurons other than daIVs are subject to *Hox* effects that ultimately impact self-righting.

However, the observation of *Hox* RNA expression in the multidendritic population does not necessarily imply *Hox* protein translation. Furthermore, we lacked information about the exact neurons in which *Antp* and *Abd-b* could be exerting their effects on self-righting, information that should aid our understanding of the sensory processing underlying self-righting. To address these open aspects, we carried out a series of fluorescence immunolabelling experiments to map the expression of *Antp* and *Abd-B* proteins in late-stage *109(2)80>mCD8::GFP* embryos to determine whether these proteins were expressed in the multidendritic population. As we had discovered that self-righting behaviour relies on precise mechanical stimulation at different regions of the body, we endeavoured to capture expression in the different clusters of the developing PNS. For

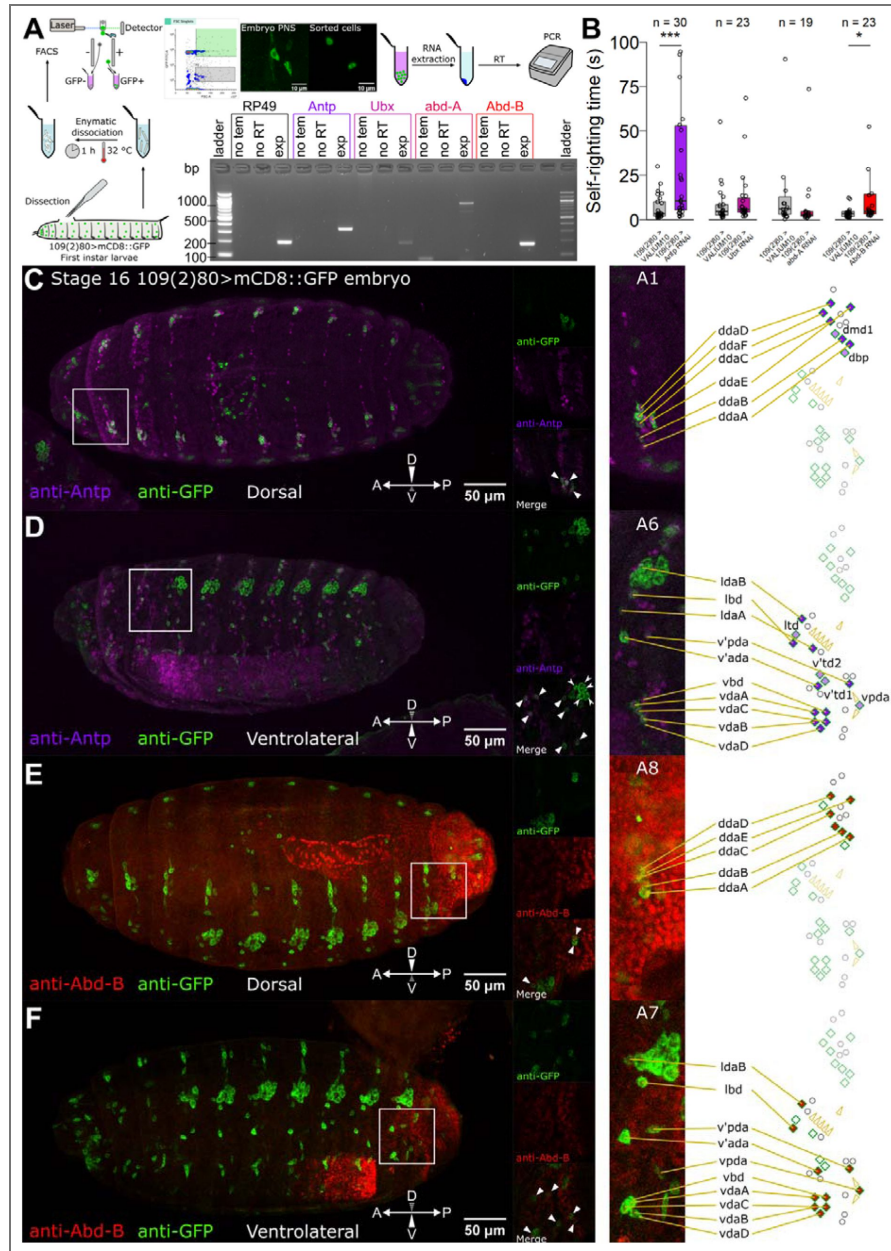


Figure 6. Hox expression in the sensory system and its influence on self-righting behaviour

A) Quantification of Hox RNA expression in larval sensory neurons. The flow diagram (beginning bottom left) shows how sensory neurons were collected from dissected first instar larvae using fluorescence-activated cell sorting (FACS). RNA was extracted from the sorted cells and reverse transcribed to DNA for amplification of Hox gene products via PCR. The photograph (bottom right) shows an agarose gel electrophoresis following RT-PCR of Hox genes *Antp*, *Ubx*, *abd-A* and *Abd-B*. For each gene, 'no tem' indicates a no template cDNA control, 'no RT' indicates a no reverse transcription control, and 'exp' indicates the experimental lane. **B)** Self-righting times of first instar larvae expressing a Hox gene RNAi construct in the 109(2)80 domain. '***' = $P < .001$, '*' = $P < .05$ for Wilcoxon rank sum tests, $n = 19-30$. **C-F)** Confocal images of immunolabelled stage 16 109(2)80>mCD8::GFP embryos. In each case, the large left panel is a maximum intensity z-projection. The white square indicates the region that is zoomed in the smaller panels to the right. These smaller panels show an individual z slice in the two separate channels and the channel overlay. Triangles indicate cells showing clear signal for Hox protein, and arrowheads indicate cells lacking signal for Hox protein. The strips on the right are zoomed sections of the z-projection, showing a range of cells in one embryonic hemisegment. The putative identities of these cells are indicated by red lines in accordance with the canonical hemisegmental diagram on the far right. **C)** Embryo immunolabelled for *Antp* and GFP, dorsal view. **D)** Embryo immunolabelled for *Antp* and GFP, ventrolateral view. **E)** Embryo immunolabelled for *Abd-B* and GFP, dorsal view. **F)** Embryo labelled for *Abd-B* and GFP, ventrolateral view.

both Hox genes, we observed the expected pattern of expression within the developing CNS, with *Antp* showing high expression in the anterior of the VNC [Figure 6D] and *Abd-b* displaying strong signal at the very posterior of the VNC [Figure 6F], providing a natural internal control for our experiments.

Analysis of the PNS pattern for *Antp* showed, unexpectedly, signal throughout the entire PNS, in the dorsal [Figure 6C] as well as the ventral and lateral clusters of multidendritic neurons [Figure 6D]. However, the intensity of the observed signal was suggestive of a trend with higher values in the anterior. With regard to specific neuronal classes, examination across z slices revealed that *Antp* was expressed in the majority of neurons labelled by 109(2)80-Gal4, save for the lateral cluster of oenocytes that also fall into this domain [Grueber et al., 2002; Klann et al., 2021]. Additionally, we were unable to precisely confirm *Antp* expression within the tracheal branching and bipolar multidendritic neurons, which could be due to the reduced expression strength of these classes in the 109(2)80-Gal4 domain compared to the dendritic arborisation neurons [Hughes & Thomas, 2007]. These observations lead us to conclude that *Antp* is likely expressed within all dendritic arborisation neurons of the PNS with a potentially modestly higher level in anterior regions.

Conversely, the expression of *Abd-b* within the PNS was more limited. While we observed expression in the dorsal [Figure 6E], ventral and lateral clusters [Figure 6F], strong signal was restricted to segments A7 and A8, mirroring the pattern of the CNS. As with *Antp*, *Abd-B* signal was observed in most neurons of those segments, suggesting a role for *Abd-B* in the posterior-most dendritic arborisation neurons. However, due to the restricted expression domain, as well as the uncharacterised nature of the multidendritic neurons in A8, we cannot assert that *Abd-B* is expressed in all the dendritic arborisation neurons of these two segments. Regardless, given our findings that self-righting relies on sensory information from the anterior, we suggest that the role of *Abd-B* in this behaviour is likely to be attributed to the regulation of motor patterns through proprioceptive feedback. Taken together, these results show that at least two Hox genes – *Antp* and *Abd-b* – are expressed within sensory neurons of the late embryo and early larva, and that this expression is key for optimal sensory function in the context of self-righting behaviour. That these two Hox genes, but not *Ubx* or *abd-A*, affect self-righting via the sensory system might suggest a role of the two termini of the animal in interpreting sensory information for complex behaviours like self-righting.

Discussion

Mapping the behavioural effects of regional stimulation in *Drosophila* larvae

The interplay between mechanical stimuli, sensory neuron activity and specific behaviours has been well-studied, with *Drosophila* research leading progress in this field [Hughes & Thomas, 2007; Ohyama et al., 2013; Titlow et al., 2014; Ohyama et al., 2015; Jovanic et al., 2016; Burgos et al., 2018; Liu et al., 2022]. Here we extend this work by examining the influences of body plan, morphology, and axial patterning on the relationship between sensory function and behaviour. Through examination of postural control, as instantiated in the highly conserved self-righting behaviour, we sought to address how localised sensory function relates to the coordinated movement of specific body parts. Using a novel manipulation technique that we coin ‘water-unlocking’, we first characterised the self-righting sequence as involving a strong movement and curvature of the anterior, which increases in magnitude over the course of the behaviour. To test how this behaviour is related to sensory contexts, we restricted substrate contact to different regions of the body, finding that anterior substrate contact on the dorsal side is required for self-righting while anterior contact at the ventral side prevents its occurrence.

Wishing to know which sensory neurons underlie this anterior precedence, we assayed self-righting under conditional inhibition of subpopulations of sensory neurons. We observed that inhibition of multidendritic neurons, in particular that of daIV neurons, led to deficits in self-righting behaviour, in agreement with previous results employing constitutive inhibition [Klann et

al., 2021 [↗](#)]. However, it remained unclear how the localised activity of these neurons might shape behavioural responses. To address this issue, we developed a new technique that we term the ‘opto-axial approach’, which involved optogenetic inhibition of groups of sensory neurons along the AP axis [Video S1]. In alignment with our previous results, we found that inhibition of multidendritic neurons in the thoracic and anterior abdominal segments led to strong deficits in self-righting behaviour, while inhibition at posterior segments had no discernible effect. These results confirm a role of anterior multidendritic activity in driving the head-dominated self-righting behaviour, and agree with prior studies observing a particular sensory sensitivity of the anterior body [Murawski et al., 2020 [↗](#)]. However, although anterior sensory function appeared to be important for self-righting, it was not clear how disrupting this activity was affecting the behavioural sequence. Using automated tracking [Video S2] of body parts along the AP axis, we found that inhibition of anterior sensory neurons produced a unique over-representation of head casting behaviour, which was strongly correlated with delays in time taken to complete self-righting. This suggests that despite the important role of head movement in self-righting, a lack of normal sensory activity at the anterior causes a switch to different behavioural sequence characterised by excessive head movement that fails to convert to the rest of the behavioural sequence. The same patterns of self-righting delays and behavioural changes were also observed for axial inhibition of daIV neurons specifically, suggesting this subpopulation of md neurons are important for inferring postural state. However, stronger effect sizes for inhibition of the whole md population also indicates that other subpopulations of the md neurons, such as the daIs or daIIs, contribute to normal self-righting completion. We speculate that given their wide dendritic arbors and ability to detect externally applied pressure [Liu et al., 2022 [↗](#)], the daIV neurons most likely detect substrate contact and allow the inference of position with respect to external surfaces. In contrast, the daI neurons, which have a known role in proprioception [Vaadia et al., 2019 [↗](#)], likely detect the body configuration such as the magnitude of bends and torsion. The combination of these different somatosensory elements is likely necessary for a typical and efficient self-righting sequence.

Finally, we questioned which genetic mechanisms might contribute to the observed patterns of anterior sensory dominance. Given the discrepancies of activity according to the AP axis, we hypothesised that the Hox genes may play a role. Through a combination of cell sorting, PCR, immunolabelling and RNAi experiments, we found that the Hox genes *Antp* and *Abd-b* are expressed in different subsets of the multidendritic sensory neurons and that typical expression levels are required for normal self-righting behaviour. Altogether, we show that the correspondence of mechanosensory stimuli and postural behaviour occurs via region-specific mechanisms that are tightly linked to body plan and its underlying genetic specification.

Exploring the relationship between body form and function via sensory biology

Our finding that anterior sensory activity is required for postural control behaviour highlights the intimate relationship between body form and function. Previous research in *Drosophila* has primarily focused on how behaviours relate to activity in different sensory cell types [Hughes & Thomas, 2007 [↗](#); Burgos et al., 2018 [↗](#); Vaadia et al., 2019 [↗](#)]. These cell types arise from differing developmental lineages and possess varying morphologies [Grueber et al., 2002 [↗](#); Singhania & Gruber, 2014], making them ideal candidates for detecting stimuli of differing modality and intensity. However, this line of investigation, though insightful, does not fully integrate the notion that behaviour is enacted through the spatial form of the body and thus also depends on the spatial configuration of the environmental stimuli that induce it.

Previous research indicated that larval responses to the same mechanosensory stimulus do depend on its location of delivery to the body [Titlow et al., 2014 [↗](#); Murawski et al., 2020 [↗](#)], as well as other contextual factors such as co-occurring stimuli [Ohshima et al., 2015 [↗](#); Jovanic et al., 2016 [↗](#)]. Neuronal manipulations have further shown that these differing responses, such as the directionality of crawling in response to a pin prick at the head or tail, depend on the localised activity of segmentally repeated interneurons that preferentially feed activity into neighbouring

motor pattern circuits [Takagi et al., 2017]. Our work extends this line of investigation by characterising the role of regional sensory components of the same cell type, enabling us to tease apart cell type specification roles from regional specific roles. In our understanding, we show for the first time that a complex behavioural sequence varies greatly according to the precise location of sensory activity. Specifically, we demonstrate that activity of anterior sensory neurons is key for the *Drosophila* larva to correct its posture with regard to the underlying substrate. That this self-righting behaviour also involves predominant movements of the head may highlight a general principle for the coordination between sensory activity and related muscle activations, indicating a possible regional, modular specialisation of neuronal circuits to reduce wiring cost and maximise efficient information flow [Rubinov, 2016; Goulas et al., 2019].

Furthermore, our finding that inhibition of anterior sensory activity does not eliminate behaviour, but instead causes a switch to increased head casting, also reflects the intimate relationship between body plan and behaviour. Despite presumably normal posterior sensory activity – and capable musculature – larvae still preferentially move with the head, a pattern we also observed during posterior-only substrate contact. We suggest this is due to the anterior dominance also observed during crawling behaviour, which is initiated with a forward grabbing with the mouth hooks [Liu et al., 2023], and which we also observed to occur under anterior ventral contact. Following from these observations, our results reflect the general principle that the sensory capacity of animals is reciprocally constrained by their behavioural repertoire, which is, in turn, further constrained by their spatial form [Salinas, 2006; Lungarella & Sporns, 2006; Molano-Mazon et al., 2023]. This goes against the notion of a one-to-one correspondence between sensory stimuli and behaviours, and, instead, points to a model in which movements are dynamically shaped by a multitude of contextual factors with spatial location being a key driver of behavioural diversity. These findings bear implications for future studies of sensory function and behaviour, since properties of a specific cell type, such as neuronal activity and synaptic connectivity, may well differ according to body localisation. Indeed, it remains an open question as to how mechanical stimuli at different locations can produce entirely different behavioural sequences. The recent ultrastructural mapping of sensory sensilla in the *Drosophila* larva [Richter et al. 2025] should pave the way to further investigations on how local stimulations trigger the complex repertoire of larval behaviours.

A novel role of the Hox genes in *Drosophila* SNs

Our finding that Hox gene expression within sensory neurons is required for normal self-righting behaviour presents a genetic mechanism by which the properties of the PNS are shaped according to position along the AP axis. In the larval CNS, expression of individual Hox proteins is constrained to localised domains along the AP axis, where they act to specify neuroblast lineages that eventually communicate with corresponding body parts in the head, thorax and abdomen [Prokop et al., 1998; Technau et al., 2006; Becker et al., 2016]. Hox expression has also been shown to be important for the specification of components of the PNS, including sensory organ precursor (SOP) formation [Gutzwiller et al., 2010] and PNS structure [Mann & Hogness, 1990; Heuer & Kaufman, 1992]. However, our work shows – in our understanding – for the first time that Hox expression is important for the normal function of the multidendritic sensory neurons. Accumulating evidence from studies in the CNS suggests that in addition to their roles in developmental specification, Hox genes also regulate post-developmental neuronal functions [Picao-Osorio 2015, Issa et al 2019, Issa et al. 2022]. For example, recent research has demonstrated that self-righting behaviour in the adult fly depends on ongoing expression of *Ubx* in NB2-3/lin15 motor neurons, which regulates plastic connectivity between these neurons and their target muscles [Issa et al., 2019]. At the larval stage, post-developmental upregulation of *Ubx* in a subset of lateral transverse (LT) motor neurons is sufficient to perturb self-righting behaviour [Picao-Osorio et al., 2015]. Based on this work, it is possible to conceive that the effects of Hox disruption we observe in the PNS could be due to a developmental effect on multidendritic neurons, an effect on neuronal physiology, or a combination of both. Indeed, previous work has shown that perturbations to Hox expression, either directly or through manipulation of Polycomb-group proteins, has a substantial impact on the dendritic structure of

the da neurons. Specifically, overexpression of several Hox genes including Ubx and Abd-A leads to under-developed dendritic arborisations, while Hox loss of function mutations promote lability of terminal dendritic branches; notably, this regulation occurs post-mitotically, suggesting an ongoing role of dendrite maintenance rather than a developmental specification [Parrish et al., 2007]. More recent work also shows that the dendritic pruning of da neurons which occurs during metamorphosis is regulated by Hox genes, with overexpression of several Hox genes including Ubx, Abd-B and Scr leading to reduced pruning [Bu et al., 2023]. Therefore, Hox expression within the da neurons is likely to regulate dendrite morphology. Interestingly, despite some of these results being specific to daIV neurons, we found no difference in self-righting times when Hox knockdown was restricted to the daIV population. This indicates that md neurons other than daIVs are subject to Hox effects that are important for self-righting. Following the results from prior work, Hox knockdown within md neurons could increase dendritic branching and thus also the sensitivity of md neurons, possibly leading to improper action selection in response to dorsal substrate contact. Visual examination of recordings suggests that in contrast to the opto-axial experiments where larvae displayed head casting, the larvae expressing Hox RNAi in md neurons showed no apparent increase in head casting but instead performed continuous forwards and backwards peristaltic waves. Speculatively, given the lack of effect in daIV neurons, this could arise from overactive daI, daII or daIII populations, leading to the selection of crawling behaviour rather than self-righting.

Despite observing expression of several Hox genes (*Antp*, *Ubx*, *abd-A* and *Abd-B*) in multidendritic neurons, behavioural phenotypes were only observed for *Antp* and *Abd-B* knockdowns. This is especially interesting given the prior findings of the role of Ubx in dendritic arborisation of da neurons [Parrish et al., 2007], and could suggest differential importance of Hox genes for various behaviours according to their spatial domains and the neurons involved. Interestingly, while we hypothesised that *Antp* would be restricted to thoracic multidendritic neurons, as is observed in the CNS [Rosales-Vega et al., 2023], we observed *Antp* expression in multidendritic neurons along the entire AP axis. While the regulatory sequences controlling *Antp* expression in the PNS have been previously characterised [Boulet & Scott, 1988], we show conclusively that *Antp* expression can extend beyond its traditionally ascribed transcriptional domain well into the entire embryonic PNS. The strong effects of *Antp* disruption on self-righting behaviour could therefore reflect an important regulatory role for *Antp* in general sensory function, which we are currently investigating. In contrast, the expression of *Abd-B* followed the expected pattern, with expression observed only in the posterior-most multidendritic neurons. Given the anterior dominance of self-righting, it is somewhat unexpected that expression changes in posterior sensory neurons could perturb the behaviour. One possibility to explain this effect is that *Abd-B* knockdown causes a misinterpretation of mechanosensory signals in posterior sensory neurons, causing a switch to a different behaviour triggered by posterior stimulation. However, given the relatively small effect of *Abd-B* knockdown, we instead suggest that the posterior sensory neurons play a mostly proprioceptive role during self-righting behaviour, contributing to the stability of posterior segments during the head-dominated self-righting sequence. It remains an open question as to exactly how Hox expression impacts self-righting behaviour via regional sensory regulation. Aside from the known effects on da neuron dendritic morphology [Parrish et al., 2007], mechanisms could include the local specification of cell identity, synapse formation, and neuronal sensitivity via the regulation of channel proteins. For example, there is evidence for a role for the anterior *Hoxd1* expression in species-specific development of nociceptive connectivity in mouse and chick [Guo et al., 2010], posterior Hox gene expression in the identity of touch-responsive neurons in *C. elegans* [Zheng et al., 2015], and *Hoxa2* expression in the somatotopic organisation of the mouse brainstem [Bechara et al., 2015]. Therefore, it is possible that proper Hox expression in *Drosophila* multidendritic neurons affects their connectivity to downstream interneurons that direct activity towards specific motorneuron circuits. Ongoing work in our laboratory is seeking to address if Hox expression in the *Drosophila* PNS affects neuronal development, regional morphology, or physiology, as well as how this expression is important for the normal execution of the extensive repertoire of behaviours displayed by the fly larva and adult.

Self-righting as an urbilaterian behaviour?

The present work has demonstrated that regional coupling between sensory function, body plan and movement is vital for an animal to properly orient itself within its environment. That righting and analogous behaviours are observed across bilaterian organisms, including invertebrates [Faisal & Matheson, 2001 [↗](#); Bilbao et al., 2018 [↗](#)], fish [Bagnall & Schoppik, 2018 [↗](#)], birds [Seal et al., 2019 [↗](#)] and mammals [Jusufi et al., 2011 [↗](#); Feather-Schussler & Ferguson, 2016 [↗](#)] raises the question of whether self-righting is an ancient behaviour. Indeed, the very nature of bilaterian organisms is such that the body is asymmetrically organised along the DV axis to facilitate specialised interactions with the environment. In this context, the ancestral bilaterian, the urbilaterian, has been suggested to have had a complex benthic adult form with AP and DV patterning, and that the key regulators of this patterning have been conserved throughout evolution [Robertis & Tejada-Muñoz, 2022]. Given the requirement for a benthic adult to be anchored via its ventral side to the seabed, we speculate that self-righting behaviour may have been present in this ancient ancestor. In this context, self-righting could represent a fundamental movement that shaped body plans throughout bilaterian evolution, whereby the ability to actively invert the DV axis promoted further specialisation of the two sides of the body. While it is well accepted that the urbilaterian possessed an anterior primitive eye of some sort [Nilsson & Arendt, 2008 [↗](#)], it is unclear to what degree other sensory *apparati* may have been specialised according to the AP axis. Future studies examining the relationship between patterning genes and PNS structure will be required to narrow down the postulated regional mechanosensory and neural specialisation of the urbilaterian.

Data availability

All data generated or analysed during this study are included in the manuscript and supporting files.

Acknowledgements

We wish to thank all members of the Alonso Lab for helpful discussions and feedback on this work. We would like to acknowledge our Sussex colleagues: Andre Chagas Maia for his advice and assistance with 3D printing of components, Yan Gu for expert support to our microscopy methods and Jonathan Wing for his help with FACS. We also wish to thank the Bloomington Drosophila Stock Center and the Vienna Drosophila Research Center for supplying many of the fly stocks used in this study. This research was funded by Leverhulme Trust Doctoral Scholarship given to WR, and a UK Medical Research Council Project Grant (MR/S011609/1) and a UK Biotechnology and Biological Sciences Research Council Project Grant (BB/Y006860/1) both awarded to CRA.

Additional files

[Supplementary Materials](#) [↗](#)

Additional information

Funding

Funder	Grant reference number	Author
UKRI Medical Research Council (MRC)	MR/S011609/1	Claudio R Alonso
UKRI Biotechnology and Biological Sciences Research Council (AFRC)	BB/Y006860/1	Claudio R Alonso
Leverhulme Trust (The Leverhulme Trust)	Doctoral Scholarship	William Roseby

Author ORCID iDs

Claudio R Alonso: <https://orcid.org/0000-0001-5761-348X>

References

- Ainsley J.A.**, Pettus J.M., Bosenko D., Gerstein C.E., Zinkevich N., Anderson M.G., Adams C.M., Welsh M.J., Johnson W.A (2003) Enhanced Locomotion Caused by Loss of the *Drosophila* DEG/ENaC Protein Pickpocket1. *Current Biology* **13**:1557-1563 [https://doi.org/10.1016/S0960-9822\(03\)00596-7](https://doi.org/10.1016/S0960-9822(03)00596-7) | [PubMed](#)
- Ashe V.M.** (2013) The righting reflex in turtles: A description and comparison. *Psychonomic Science* **20**:150-152 <https://doi.org/10.3758/BF03335647>
- Bagnall M.W.**, Schoppik D (2018) Development of vestibular behaviors in zebrafish. *Current Opinion in Neurobiology* **53**:83-89 <https://doi.org/10.1016/j.conb.2018.06.004> | [PubMed](#)
- Bechara A.**, Laumonnerie C., Vilain N., Kratochwil C.F., Cankovic V., Maiorano N.A., Kirschmann M.A., Ducret S., Rijli F.M (2015) *Hoxa2* Selects Barrelette Neuron Identity and Connectivity in the Mouse Somatosensory Brainstem. *Cell Reports* **13**:783-797 <https://doi.org/10.1016/j.celrep.2015.09.031> | [PubMed](#)
- Becker H.**, Renner S., Technau G.M., Berger C (2016) Cell-Autonomous and Non-cell-autonomous Function of Hox Genes Specify Segmental Neuroblast Identity in the Gnathal Region of the Embryonic CNS in *Drosophila*. *PLoS genetics* **12**:e1005961 <https://doi.org/10.1371/journal.pgen.1005961> | [PubMed](#)
- Bilbao A.**, Patel A.K., Rahman M., Vanapalli S.A., Blawdziewicz J (2018) Roll maneuvers are essential for active reorientation of *Caenorhabditis elegans* in 3D media. *Proceedings of the National Academy of Sciences of the United States of America* **155**:E3616-E3625 <https://doi.org/10.1073/pnas.1706754115> | [PubMed](#)
- Boulet A.M.**, Scott M.P (1988) Control elements of the P2 promoter of the Antennapedia gene. *Genes & Development* **2**:1600-1614 <https://doi.org/10.1101/gad.2.12a.1600> | [PubMed](#)
- Burgos A.**, Honjo K., Ohyama T., Qian C.S., Shin G.J., Gohl D.M., Silies M., Tracey W.D., Zlatić M., Cardona A., et al. (2018) Nociceptive interneurons control modular motor pathways to promote escape behavior in *Drosophila*. *eLife* **7**:e26016 <https://doi.org/10.7554/eLife.26016> | [PubMed](#)
- Caldwell J.C.**, Miller M.M., Wing S., Soll D.R., Eberl D.F (2003) Dynamic analysis of larval locomotion in *Drosophila* chordotonal organ mutants. *Proceedings of the National Academy of Sciences* **100**:16053-16058 <https://doi.org/10.1073/pnas.2535546100> | [PubMed](#)
- Cooney P.C.**, Huang Y., Li W., Perera D.M., Hormigo R., Tabachnik T., Godage I.S., Hillman E.M.C., Grueber W.B., Zarin A.A (2023) Neuromuscular basis of *Drosophila* larval rolling escape behavior. *Proceedings of the National Academy of Sciences of the United States of America* **120**:e2303641120 <https://doi.org/10.1073/pnas.2303641120> | [PubMed](#)
- De Robertis E.M.**, Sasai Y. (1996) A common plan for dorsoventral patterning in Bilateria. *Nature* **380**:37-40 <https://doi.org/10.1038/380037a0> | [PubMed](#)
- De Robertis E.M.**, Tejeda-Muñoz N. (2022) Evo-Devo of *Urbilateria* and its larval forms. *Developmental Biology* **487**:10-20 <https://doi.org/10.1016/j.ydbio.2022.04.003> | [PubMed](#)
- Evans A.**, Ferrer A.J., Fradkov E., Shomar J.W., Forer J., Klein M (2023) Temperature sensitivity and temperature response across development in the *Drosophila* larva. *Frontiers in Molecular Neuroscience* **16** <https://doi.org/10.3389/fnmol.2023.1275469> | [PubMed](#)
- Faisal A.A.**, Matheson T (2001) Coordinated Righting Behaviour in Locusts. *Journal of Experimental Biology* **204**:637-648 <https://doi.org/10.1242/jeb.204.4.637> | [PubMed](#)
- Feather-Schussler D.N.**, Ferguson T.S (2016) A Battery of Motor Tests in a Neonatal Mouse Model of Cerebral Palsy. *Journal of Visualized Experiments: JoVE* 53569 <https://doi.org/10.3791/53569> | [PubMed](#)
- Fushiki A.**, Kohsaka H., Nose A (2013) Role of Sensory Experience in Functional Development of *Drosophila* Motor Circuits. *PLOS One* **8**:e62199 <https://doi.org/10.1371/journal.pone.0062199> | [PubMed](#)

- Gao F.-B., Brenman J.E., Jan L.Y., Jan Y.N (1999) Genes regulating dendritic outgrowth, branching, and routing in *Drosophila*. *Genes & Development* **13**:2549-2561 <https://doi.org/10.1101/gad.13.19.2549> | PubMed
- Gorczyca D.A., Younger S., Meltzer S., Kim S.E., Cheng L., Song W., Lee H.Y., Jan L.Y., Jan Y.N (2014) Identification of Ppk26, a DEG/ENaC Channel Functioning with Ppk1 in a Mutually Dependent Manner to Guide Locomotion Behavior in *Drosophila*. *Cell Reports* **9**:1446-1458 <https://doi.org/10.1016/j.celrep.2014.10.034> | PubMed
- Govorunova E.G., Sineshchekov O.A., Janz R., Liu X., Spudich J.L (2015) Natural light-gated anion channels: A family of microbial rhodopsins for advanced optogenetics. *Science* **349**:647-650 <https://doi.org/10.1126/science.aaa7484> | PubMed
- Grueber W.B., Jan L.Y., Jan Y.N (2002) Tiling of the *Drosophila* epidermis by multidendritic sensory neurons. *Development* **129**:2867-2878 <https://doi.org/10.1242/dev.129.12.2867> | PubMed
- Guo T., Mandai K., Condie B.G., Wickramasinghe S.R., Capecchi M.R., Ginty D.D (2011) An evolving NGF-Hoxd1 signaling pathway mediates development of divergent neural circuits in vertebrates. *Nature Neuroscience* **14**:31-36 <https://doi.org/10.1038/nn.2710> | PubMed
- Gutzwiller L.M., Witt L.M., Gresser A.L., Burns K.A., Cook T.A., Gebelein B (2010) Proneural and abdominal Hox inputs synergize to promote sensory organ formation in the *Drosophila* abdomen. *Developmental Biology* **348**:231-243 <https://doi.org/10.1016/j.ydbio.2010.09.014> | PubMed
- Hartenstein V (1988) Development of *Drosophila* larval sensory organs: spatiotemporal pattern of sensory neurones, peripheral axonal pathways and sensilla differentiation. *Development* **102**:869-886 <https://doi.org/10.1242/dev.102.4.869>
- Harzer H., Berger C., Conder R., Schmauss G., Knoblich J.A (2013) FACS purification of *Drosophila* larval neuroblasts for next-generation sequencing. *Nature Protocols* **8**:1088-1099 <https://doi.org/10.1038/nprot.2013.062> | PubMed
- Heuer J.G., Kaufman T.C (1992) Homeotic genes have specific functional roles in the establishment of the *Drosophila* embryonic peripheral nervous system. *Development (Cambridge, England)* **115**:35-47 <https://doi.org/10.1242/dev.115.1.35> | PubMed
- Hughes C.L., Thomas J.B (2007) A sensory feedback circuit coordinates muscle activity in *Drosophila*. *Molecular and Cellular Neuroscience* **35**:383-396 <https://doi.org/10.1016/j.mcn.2007.04.001> | PubMed
- Hwang R.Y., Zhong L., Xu Y., Johnson T., Zhang F., Deisseroth K., Tracey W.D (2007) Nociceptive Neurons Protect *Drosophila* Larvae from Parasitoid Wasps. *Current Biology* **17**:2105-2116 <https://doi.org/10.1016/j.cub.2007.11.029> | PubMed
- Issa A.R., Picao-Osorio J., Rito N., Chiappe M.E., Alonso C.R (2019) A Single MicroRNA-Hox Gene Module Controls Equivalent Movements in Biomechanically Distinct Forms of *Drosophila*. *Current biology: CB* **29**:2665-2675.e4. <https://doi.org/10.1016/j.cub.2019.06.082> | PubMed
- Jang W., Lee S., Choi S.-I., Chae H.-S., Han J., Jo H., Hwang S.W., Park C.-S., Kim C (2019) Impairment of proprioceptive movement and mechanical nociception in *Drosophila melanogaster* larvae lacking Ppk30, a *Drosophila* member of the Degenerin/Epithelial Sodium Channel family. *Genes, Brain, and Behavior* **18**:e12545 <https://doi.org/10.1111/gbb.12545> | PubMed
- Jonaitis J., Hibbard K.L., Layte K.M., Hiramoto A., Cardona A., Truman J.W., Nose A., Zwart M.F., Pulver S.R. (2024) Steering From the Rear: Coordination of Central Pattern Generators Underlying Navigation by Ascending Interneurons. *bioRxiv* 2024.06.17.598162 <https://doi.org/10.1101/2024.06.17.598162>
- Jovanic T., Schneider-Mizell C.M., Shao M., Masson J.-B., Denisov G., Fetter R.D., Menseh B.D., Truman J.W., Cardona A., Zlatić M (2016) Competitive Disinhibition Mediates Behavioral Choice and Sequences in *Drosophila*. *Cell* **167**:858-870.e19. <https://doi.org/10.1016/j.cell.2016.09.009> | PubMed
- Jusufi A., Zeng Y., Full R.J., Dudley R (2011) Aerial Righting Reflexes in Flightless Animals. *Integrative and Comparative Biology* **51**:937-943 <https://doi.org/10.1093/icb/icr114> | PubMed

- Kitamoto T** (2001) Conditional modification of behavior in *Drosophila* by targeted expression of a temperature-sensitive shibire allele in defined neurons. *Journal of Neurobiology* **47**:81-92 <https://doi.org/10.1002/neu.1018> | [PubMed](#)
- Klann M., Issa A.R., Pinho S., Alonso C.R** (2021) MicroRNA-Dependent Control of Sensory Neuron Function Regulates Posture Behavior in *Drosophila*. *The Journal of Neuroscience: The Official Journal of the Society for Neuroscience* **41**:8297-8308 <https://doi.org/10.1523/JNEUROSCI.0081-21.2021> | [PubMed](#)
- Liu Y., Hasegawa E., Nose A., Zwart M.F., Kohsaka H** (2023) Synchronous multi-segmental activity between metachronal waves controls locomotion speed in *Drosophila* larvae. *eLife* **12**:e83328 <https://doi.org/10.7554/eLife.83328> | [PubMed](#)
- Liu Z., Wu M.-H., Wang Q.-X., Lin S.-Z., Feng X.-Q., Li B., Liang X** (2022) *Drosophila* mechanical nociceptors preferentially sense localized poking. *eLife* **11**:e76574 <https://doi.org/10.7554/eLife.76574> | [PubMed](#)
- Loveless J., Garner A., Issa A.R., Roberts R.J.V., Webb B., Prieto-Godino L.L., Ohyama T., Alonso C.R.** (2021) A physical theory of movement in small animals. *bioRxiv* 2020.08.25.266163 <https://doi.org/10.1101/2020.08.25.266163>
- Mallo M., Alonso C.R** (2013) The regulation of Hox gene expression during animal development. *Development (Cambridge, England)* **140**:3951-3963 <https://doi.org/10.1242/dev.068346> | [PubMed](#)
- Mann R.S., Hogness D.S** (1990) Functional dissection of ultrabithorax proteins in *D. melanogaster*. *Cell* **60**:597-610 [https://doi.org/10.1016/0092-8674\(90\)90663-Y](https://doi.org/10.1016/0092-8674(90)90663-Y) | [PubMed](#)
- Mathis A., Mamidanna P., Cury K.M., Abe T., Murthy V.N., Mathis M.W., Bethge M** (2018) DeepLabCut: markerless pose estimation of user-defined body parts with deep learning. *Nature Neuroscience* **21**:1281-1289 <https://doi.org/10.1038/s41593-018-0209-y> | [PubMed](#)
- McGraw M.B** (1941) Neural maturation of the infant as exemplified in the righting reflex, or rolling from a dorsal to a prone position. *The Journal of Pediatrics* **18**:385-394 [https://doi.org/10.1016/S0022-3476\(41\)80189-9](https://doi.org/10.1016/S0022-3476(41)80189-9)
- Murawski C., Pulver S.R., Gather M.C** (2020) Segment-specific optogenetic stimulation in *Drosophila melanogaster* with linear arrays of organic light-emitting diodes. *Nature Communications* **11**:6248 <https://doi.org/10.1038/s41467-020-20013-6> | [PubMed](#)
- Nilsson D.-E., Arendt D** (2008) Eye evolution: the blurry beginning. *Current biology: CB* **18**:R1096-1098 <https://doi.org/10.1016/j.cub.2008.10.025> | [PubMed](#)
- Ohyama T., Jovanic T., Denisov G., Dang T.C., Hoffmann D., Kerr R.A., Zlatić M** (2013) High-Throughput Analysis of Stimulus-Evoked Behaviors in *Drosophila* Larva Reveals Multiple Modality-Specific Escape Strategies. *PLOS One* **8**:e71706 <https://doi.org/10.1371/journal.pone.0071706> | [PubMed](#)
- Ohyama T., Schneider-Mizell C.M., Fetter R.D., Aleman J.V., Franconville R., Rivera-Alba M., Mensh B.D., Branson K.M., Simpson J.H., Truman J.W., et al.** (2015) A multilevel multimodal circuit enhances action selection in *Drosophila*. *Nature* **520**:633-639 <https://doi.org/10.1038/nature14297> | [PubMed](#)
- Penn D., Jane Brockmann H** (1995) Age-biased stranding and righting in male horseshoe crabs, *Limulus polyphemus*. *Animal Behaviour* **49**:1531-1539 [https://doi.org/10.1016/0003-3472\(95\)90074-8](https://doi.org/10.1016/0003-3472(95)90074-8)
- Picao-Osorio J., Johnston J., Landgraf M., Berni J., Alonso C.R** (2015) MicroRNA-encoded behavior in *Drosophila*. *Science* **350**:815-820 <https://doi.org/10.1126/science.aad0217> | [PubMed](#)
- Picao-Osorio J., Lago-Baldaia I., Patraquim P., Alonso C.R** (2017) Pervasive Behavioral Effects of MicroRNA Regulation in *Drosophila*. *Genetics* **206**:1535-1548 <https://doi.org/10.1534/genetics.116.195776> | [PubMed](#)
- Prokop A., Bray S., Harrison E., Technau G.M** (1998) Homeotic regulation of segment-specific differences in neuroblast numbers and proliferation in the *Drosophila* central nervous system. *Mechanisms of Development* **74**:99-110 [https://doi.org/10.1016/s0925-4773\(98\)00068-9](https://doi.org/10.1016/s0925-4773(98)00068-9) | [PubMed](#)

- Raouf Issa A., A. C. Menzies J., Padmanabhan A., Alonso C.R. (2022) A novel post-developmental role of the Hox genes underlies normal adult behavior. *Proceedings of the National Academy of Sciences* **119**:e2209531119 <https://doi.org/10.1073/pnas.2209531119> | PubMed
- R Core Team (2024) R: A Language and Environment for Statistical Computing. <https://www.R-project.org/>
- Richter V., Rist A., Kislinger G, Laumann M, Schoofs A., Miroschnikow A., Pankratz M.J., Cardona A., Thum A.S. (2025) Morphology and ultrastructure of external sense organs of *Drosophila* larvae. *eLife* <https://doi.org/10.7554/eLife.91155.3>
- Rosales-Vega M., Reséndez-Pérez D., Vázquez M (2024) Antennapedia: The complexity of a master developmental transcription factor. *Genesis (New York, N.Y.: 2000)* **62**:e23561 <https://doi.org/10.1002/dvg.23561> | PubMed
- Seal H.E., Lilian S.J., Popratiloff A., Hirsch J.C., Peusner K.D (2019) Implementing the chick embryo model to study vestibular developmental disorders. *Journal of Neurophysiology* **122**:2272-2283 <https://doi.org/10.1152/jn.00434.2019> | PubMed
- Siegel D.N., Siddicky S.F., Davis W.D., Mannen E.M (2024) Muscle activation and coordinated movements of infant rolling. *Journal of Biomechanics* **162**:111890 <https://doi.org/10.1016/j.jbiomech.2023.111890> | PubMed
- Singhania A., Grueber W.B (2014) Development of the embryonic and larval peripheral nervous system of *Drosophila*. *WIREs Developmental Biology* **3**:193-210 <https://doi.org/10.1002/wdev.135> | PubMed
- Sterling P (2015) Principles of Efficient Wiring. In: Sterling P., Laughlin S. (Eds). *Principles of Neural Design* **0** The MIT Press. <https://doi.org/10.7551/mitpress/9780262028707.003.0013>
- Takagi S., Cocanougher B.T., Niki S., Miyamoto D., Kohsaka H., Kazama H., Fetter R.D., Truman J.W., Zlatic M., Cardona A., et al. (2017) Divergent Connectivity of Homologous Command-like Neurons Mediates Segment-Specific Touch Responses in *Drosophila*. *Neuron* **96**:1373-1387.e6. <https://doi.org/10.1016/j.neuron.2017.10.030> | PubMed
- Technau G.M., Berger C., Urbach R (2006) Generation of cell diversity and segmental pattern in the embryonic central nervous system of *Drosophila*. *Developmental Dynamics: An Official Publication of the American Association of Anatomists* **235**:861-869 <https://doi.org/10.1002/dvdy.20566> | PubMed
- Teitelbaum P., Teitelbaum O., Nye J., Fryman J., Maurer R.G (1998) Movement analysis in infancy may be useful for early diagnosis of autism. *Proceedings of the National Academy of Sciences* **95**:13982-13987 <https://doi.org/10.1073/pnas.95.23.13982> | PubMed
- Titlow J.S., Rice J., Majeed Z.R., Holsopple E., Biecker S., Cooper R.L (2014) Anatomical and genotype-specific mechanosensory responses in *Drosophila melanogaster* larvae. *Neuroscience Research* **83**:54-63 <https://doi.org/10.1016/j.neures.2014.04.003> | PubMed
- Tracey W.D., Wilson R.I., Laurent G., Benzer S (2003) painless, a *Drosophila* Gene Essential for Nociception. *Cell* **113**:261-273 [https://doi.org/10.1016/S0092-8674\(03\)00272-1](https://doi.org/10.1016/S0092-8674(03)00272-1) | PubMed
- Tsubouchi A., Caldwell J.C., Tracey W.D (2012) Dendritic Filopodia, Ripped Pocket, NOMPC, and NMDARs Contribute to the Sense of Touch in *Drosophila* Larvae. *Current Biology* **22**:2124-2134 <https://doi.org/10.1016/j.cub.2012.09.019> | PubMed
- Vaadia R.D., Li W., Voleti V., Singhania A., Hillman E.M.C., Grueber W.B (2019) Characterization of Proprioceptive System Dynamics in Behaving *Drosophila* Larvae Using High-Speed Volumetric Microscopy. *Current Biology* **29**:935-944.e4. <https://doi.org/10.1016/j.cub.2019.01.060> | PubMed
- Yan Z., Zhang W., He Y., Gorczyca D., Xiang Y., Cheng L.E., Meltzer S., Jan L.Y., Jan Y.N (2013) *Drosophila* NOMPC is a mechanotransduction channel subunit for gentle-touch sensation. *Nature* **493**:221-225 <https://doi.org/10.1038/nature11685> | PubMed
- Zheng C., Diaz-Cuadros M., Chalfie M (2015) Hox Genes Promote Neuronal Subtype Diversification through Posterior Induction in *Caenorhabditis elegans*. *Neuron* **88**:514-527 <https://doi.org/10.1016/j.neuron.2015.09.049> | PubMed

Peer reviews

Reviewer #1 (Public review):

Summary:

Roseby and colleagues report on a body region-specific sensory control of the fly larval righting response, a body contortion performed by fly larvae to correct their posture from an inverted (dorsal side down) position. This is an important topic because of the general need for animals to locomote in the correct orientation and the clever and broadly useful methodologies used in this paper to uncover the sensory triggers for the behavior, including a body region-specific optogenetic approach along different axial positions of the larva, region-specific manipulation of surface contacts with the substrate, and a 'water unlocking' technique to initiate righting behaviors, all strengths of the manuscript. The authors found that multidendritic neurons, particularly the daIV neurons, are necessary for righting behavior. The contribution of daIV neurons had been shown by the authors in a prior paper (Klann et al, 2021), but that study had used constitutive neuronal silencing. Here the authors used acute inactivation to confirm this finding. Additionally, the authors describe an important role for anterior sensory neurons. They move on to test the genetic basis for righting behavior and, consistent with the regional specificity they observe, implicate sensory neuron expression of Hox genes *Antennapedia* and *Abdominal-b* in self-righting.

Strengths:

Strengths of this paper include the important question addressed and the elegant and innovative combination of methods, which led to clear insights into the sensory biology of self-righting and links between body plan and nervous system function that will be useful for others in the field. The manuscript is very clearly written and couched in interesting biology.

Limitations:

There are several important questions for future study that, left unresolved, do not diminish the significance of this manuscript. These include the cellular and developmental basis for Hox gene action, the contributions of dorsal and ventral regions of the animal in righting, and the regional contributions of other sensory cell types in the righting response.

Comments on revised version.

The authors have addressed my major concerns.

<https://doi.org/10.7554/eLife.108505.2.sa2>

Reviewer #2 (Public review):

Summary

This work explores the relationship between body structure and behavior by studying self-righting in *Drosophila* larvae, a conserved behavior that restores proper orientation when turned upside-down. The authors first introduce a novel "water unlocking" approach to induce self-righting behavior in a controlled manner. Then, they develop a method for region-specific inhibition of sensory neurons revealing that anterior, but not posterior, sensory neurons are essential for proper self-righting. Deep-learning-based behavioral analysis shows that anterior inhibition prolongs self-righting by shifting head movement patterns, indicating a behavioral switch rather than a mere delay. Additional genetic and molecular experiments demonstrate that specific Hox genes are necessary in sensory

neurons, underscoring how developmental patterning genes shape region-specific sensory mechanisms that enable adaptive motor behaviors.

Strengths

The work by Roseby et al. is notable for its elegant experimental design, the development of innovative methods that are likely to benefit the fly behavior community, and the strong experimental support for its conclusions. The manuscript is clearly written, well structured, and presents thoughtfully designed experiments that have been further improved in the revised version. This updated manuscript includes a comprehensive set of behavioral experiments using an additional Gal4 line (ppk-Gal4), which yields confirmatory results and strengthens support for the original hypothesis. It also incorporates quantification of Gal4 line strength, improvements to existing figures, the addition of new figures, and overall refinement of the text.

Weakness:

A remaining limitation of this manuscript is the lack of a cellular and mechanistic analysis explaining how Hox genes give rise to the observed behavioral phenotypes. The authors note that this question is being addressed in an ongoing follow-up study, which will expand the project to examine the roles of all Hox genes across the sensory system and to characterize their expression patterns within each of its subcomponents, with the aim of providing mechanistic insight. I look forward to seeing this work in a future manuscript.

Comments on revised version.

I have no further recommendations for the authors; most of my comments and questions have been satisfactorily addressed.

<https://doi.org/10.7554/eLife.108505.2.sa1>

Author response:

The following is the authors' response to the original reviews.

Public Reviews:

Reviewer #1 (Public review):

Strengths:

Strengths of this paper include the important question addressed and the elegant and innovative combination of methods, which led to clear insights into the sensory biology of self-righting, and that will be useful for others in the field. This is a substantial contribution to understanding how animals correct their body position. The manuscript is very clearly written and couched in interesting biology.

Limitations:

(1.1) The interpretation of functional experiments is complicated by the proposed excitatory and inhibitory roles of dorsal and ventral sensory neuron activity, respectively. So, while silencing of an excitatory (dorsal) element might slow righting, silencing of inputs that inhibit righting could speed the behavior. Silencing them together, as is done here, could nullify or mask important D-V-specific roles. Selective manipulation of cells along the D-V axis could help address this caveat.

We highly appreciate the thoughtful comments by Rev1 pointing out the relative simplicity of our current inferences regarding the role of dorsal vs. ventral substrate contact, and agree

with the suggestion that cells along the DV axis could have diverse roles in their contribution to self-righting. In this context, we wish to point out two aspects, one theoretical and one practical. Regarding theory, our view is that this may not be a simple case of “excitation vs. inhibition”, but rather one in which the coordinated and dynamic activity of distributed sensory neurons promotes differential action selection in alignment with environmental conditions – a framework that could involve many different behaviours with a still uncertain level of granularity (e.g., is self-righting different if the larva is rotated to 160° instead of exactly 180°?). Regarding the practical aspect, while this area represents a fascinating point for future investigation, it is currently limited by technological development, particularly in the context of this study where a relatively low-cost implementation has been used to probe the AP axis. Investigation of the DV axis would require further technological development, since optogenetic light would need to be precisely delivered from the side rather than from underneath, with a greater degree of resolution compared to the AP axis given the much smaller width of the larva (~120-140µm) relative to its length (~550-600µm). Therefore, whilst we appreciate these comments and suggestion, we believe this line of experiments is ideal for a follow-up investigation, rather than being implemented in the current study.

(1.2) Prior studies from the authors implicated daIV neurons in the righting response. One of the main advances of the current manuscript is the clever demonstration of region-specific roles of sensory input. However, this is only confirmed with a general md driver, 190(2)80, and not with the subsetspecific Gal4, so it is not clear if daIV sensory neurons are also acting in a regionally-specific manner along the A-P axis.

To address this interesting and important comment by Rev1 we have carried out a new experiment using an alternative driver to *109(2)80-Gal4* and testing the impact of these manipulations on larval behaviour. The revised version of our MS includes a new figure Supp Fig S3 which shows self-righting times when using the *ppk-Gal4* driver with the opto-axial technique. As observed with the *109(2)80-Gal4* driver, self-righting was delayed in anterior but not posterior inhibition conditions, suggesting the daIV neurons act in a region-specific manner to trigger postural control behaviour.

We have also conducted a head casting analysis in the *ppk* domain; in another new figure, Supp Fig S7, we also show that head casting behaviour is also increased in the same manner as with the *109(2)80-Gal4* driver.

These new panels and figures are cited within the sub sections entitled “Optogenetic inhibition of anterior but not posterior multidendritic neurons delays self-righting” and “Inhibition of anterior multidendritic neurons is associated with increased head casting during self-righting”, on pages 25 and 28, respectively. We are grateful to Rev1 for this suggestion, which we consider qualitatively improves our paper.

(1.3) The manuscript is narrowly focused on sensory neurons that initiate righting, which limits the advance given the known roles for daIV neurons in righting. With the suite of innovative new tools, there is a missed opportunity to gain a more general understanding of how sensory neurons contribute to the righting response, including promoting and inhibiting righting in different regions of the larva, as well as aspects of proprioceptive sensing that could be necessary for righting and account for some of the observed effects of 109(2)80.

Once again, we appreciate this interesting comment by Rev1. We feel our study provides novelty in understanding how sensory neurons in different body regions contribute to the induction of the behaviour. We developed new technology to show that the activity of anterior sensory neurons is essential for normal righting and inhibiting this activity leads to a switch to a different behavioural regime. We feel this represents a substantial advancement in our understanding of how this behaviour is initiated that has not been previously described. Whilst we also appreciate there is likely to be a substantial role of proprioception

in self-righting behaviour, our work here focuses on the external stimuli that elicit self-righting, as a detailed understanding of proprioception would be out of scope and require the development of further techniques to manipulate and measure larval posture. As detailed in the above comment, we feel that the more targeted investigation of daIV neurons can also shed some light on the cell-type specificity and inputs to the self-righting induction process.

(1.4) Although the authors observe an influence of Hox genes in righting, the possible mechanisms are not pursued, resulting in an unsatisfying conclusion that these genes are somehow involved in a certain region-specific behavior by their region-specific expression. Are the cells properly maintained upon knockdown? Are axon or dendrite morphologies of the cells disrupted upon knockdown?

We agree with this comment in that further investigating the effects of Hox expression on localised aspects of the sensory system poses an interesting line of investigation. Indeed, we are currently conducting a full scale analysis of Hox gene effects across the sensory field. As things stand, it is not clear how Hox gene expression could affect local sensory processes, a mechanism which could involve morphological changes, changes in neuronal excitability (e.g. due to changes in channel expression), synapse formation and/or efficiency, cell development and identity, and/or combinations of these effects, amongst other possibilities. It is clear that a complete and satisfying investigation of this mechanism for each of the Hox genes would pose a substantial amount of work so, while we acknowledge the merit of Rev1's comment, we consider that adding a cellular-mechanistic analysis of Hox effects is out of scope for the present study and shall constitute a central matter for a followup study emerging from current projects. We think that our data on Hox expression/function as reported here should serve to open up the analysis of genetic regulation of local sensory function, an area in which we are currently working very actively.

(1.5) There could be many reasons for delays in righting behavior in the various manipulations, including ineffective sensory 'triggering', incoherent muscle contraction patterns, initiation of inappropriate behaviors that interfere with righting sequencing, and deficits in sensing body position. The authors show that delays in righting upon silencing of 109(2)80 are caused by a switch to head casting behavior. Is this also the case for silencing of daIV neurons, Hox RNAi experiments, and silencing of CO neurons? Does daIII silencing reduce head casting to lead to faster righting responses?

This is an insightful comment. In the revised version of the manuscript, we do indeed show that anterior inhibition of daIV neurons leads to the same head casting behaviour as with the 109(2)80 domain, which we interpret as an inability of the larvae to sense the underlying substrate (see page 28). We hope the new data addresses this comment, at least to an extent. While we acknowledge it would also be insightful to run this behavioural analysis for other experimental conditions, such as the daIII inhibition and Hox RNAi lines, these experiments pose a specific technical difficulty: the behavioural analysis relies on a deep neural network (DNN) which was trained solely on recordings of the opto-axial technique, meaning it does not translate well to other experimental situations. This problem is further compounded by the use of L1 larvae, which means recording resolution is insufficient to accurately define the body landmarks used in the posture tracking at a smaller scale. Therefore, the recourse for identifying behavioural changes is manual observation, which we feel is too inconsistent to address a quantitative question like this.

(1.6) 109(2)80 is expressed in a number of central neurons, so at least some of the righting phenotype with this line could be due to silenced neurons in the CNS. This should at least be acknowledged in the manuscript and controlled for, if possible, with other Gal4 lines.

We thank the reviewer for making this interesting comment. We have added a phrase to the section "Conditional inhibition of multidendritic neurons delays self-righting" (p21) which

acknowledges the presence of 109(2)80 expression in the CNS (as reported by Hughes and Thomas). We agree that ideally, a variety of sensory Gal4 lines would be used to check for consistency of the effects. However, it is also important to note that 109(2)80 is one of the only available Gal4 lines with near sole md neuron expression, as other Gal4s also drive expression strongly in external sensory cells for example. Thus, re-running experiments with these other lines – which would involve a substantial investment of time and resources – would not be an ideal strategy. We feel that the new observation of (very) similar axial results using the ppk-Gal4, which does express solely in the daIV neurons, better helps to confirm the specificity of the findings to multidendritic neurons.

Other points:

(1.7) Interpretation of roles of Hox gene expression and function in righting response should consider previous data on Hox expression and function in multidendritic neurons reported by Parrish et al. Genes and Development, 2007.

We thank Rev1 for pointing out this study, which is definitely important to discuss given our results on Hox genes. To address this gap, we have added an additional paragraph in the Discussion (p37) to discuss the documented effects of Hox genes on da neuron dendritic morphology and how our results can be interpreted in light of this.

(1.8) The daIII silencing phenotype could conceivably be explained if these neurons act as the ventral inhibitors. Do the authors have evidence for or against such roles?

This is another interesting suggestion. If the daIII neurons were to fulfil this role, then in theory, their inhibition would result in self-righting behaviour under conditions of combined dorsal and ventral substrate contact. This is not an experiment we performed, so we are currently unable to confirm or rule out this possibility. However, we note from casual observation that daIII inhibition does not cause larvae to spontaneously self-right. As mentioned above, our view is not one in which the system has “dorsal/ventral stimulators/inhibitors” for a given behaviour, but that action selection proceeds according to a coordination of many (dynamic) contextual clues. Given the new results with the axial inhibition of daIV neurons (see above) it might be more parsimonious to suggest that these “tiling” neurons are primarily responsible for detecting substrate contact around the full circumference of the animal, rather than this involving different cell types according to the different sides of the body.

Reviewer #2 (Public review):

Strengths:

The work of Roseby et al. does what it says on the tin. The experimental design is elegant, introducing innovative methods that will likely benefit the fly behavior community, and the results are robustly supported, without overstatement.

Weaknesses:

The manuscript is clearly written, flows smoothly, and features well-designed experiments. Nevertheless, there are areas that could be improved. Below is a list of suggestions and questions that, if addressed, would strengthen this work:

(2.1) Figure 1A illustrates the sequence of self-righting behavior in a first instar larva, while the experiments in the same figure are performed on third instar larvae. It would be helpful to clarify whether the sequence of self-righting movements differs between larval stages. Later on in the manuscript, experiments are conducted on first instar larvae without explanation for the choice of stage. Providing the rationale for using different larval stages would improve clarity.

This is a very interesting point raised by Rev2. Most of our previous work on self-righting (e.g. PicaoOsorio et al. 2015 Science; Picao-Osorio, Baldaia et al. 2017 Genetics; Klann et al. 2021 Journal of Neuroscience) was focused on the first instar larva (L1) because this early stage: (i) represents the simplest form of all larval stages, (ii) allows meaningful comparisons with late embryonic processes guiding the development and physiology of the nervous system, (iii) captures the system in a relatively naïve state, that had limited if any exposure to external stimuli. Although these attributes remain valid for the investigation of the sensory stimuli that trigger self-righting, the implementation of the necessary regional physical measurements and manipulations used in this study (surface contact, opto-axial technique, deep neural network analysis) would be impossible to implement in the early forms of the larva simply due to its reduced size. Due to this, we employed L3s, which due to their larger dimensions enabled the development and use of the sophisticated regional stimulation techniques reported here. Yet, as Rev2 rightly points out, we return to the late embryo and early L1 at the point of conducting gene expression analyses as these are optimised for those early stages. The selection of larval stage according to experiment relies on the fact that all forms of the larva display self-righting (Issa, Picao-Osorio, et al. 2019 Current Biology), that SR does not differ according to larval stage and that the characterisation of the structure of the nervous system across larval stages has shown a large level of similarity and consistent topographically arranged connectivity between identified neurons (Gerhard et al. 2017 eLife).

(2.2) What was the genotype of the larvae used for the initial behavioral characterization (Figure 1)? It is assumed they were wild type or w¹¹¹⁸, but this should be stated explicitly. This also raises the question of whether different wild-type strains exhibit this behavior consistently or if there is variability among them. Has this been tested?

Thank you to the reviewer for pointing this out. The genotype for Figure 1 was *w¹¹¹⁸*; this has now been added to the figure legend and the results section – thank you to Rev2 for pointing this out. Although in this study we did not explicitly compare self-righting (SR) performance in wild type/control genotypes (as we are internally consistent in using *w¹¹¹⁸*) based on previous data collected in our lab we know that self-righting times are similar and very consistent amongst inbred control lines such as *w¹¹¹⁸*, *yw*, and *Oregon Red*. Furthermore, we can also add that when comparing SR times between these inbred populations with a highly polymorphic outbred *Drosophila* population (Martins et al. 2013 PLoS Pathogens) we observed that their SR time (i.e. 6.14s ± 1.06) was not significantly different from the inbred lines (p<0.05, U test) (Picao-Osorio, J. 2014 Doctoral Thesis, Chapter 4, p112).

(2.3) Could the observed slight leftward bias in movement angles of the tail (Figure 1I and S1) be related to the experimental setup, for example, the way water is added during the unlocking procedure? It would be helpful to include some speculation on whether the authors believe this preference to be endogenous or potentially a technical artifact.

This is an interesting comment, and we recognise that lateral manipulation biases in self-righting could indeed reflect experimental limitations or biological tendencies. At this point we cannot interpret these results as formal evidence of chirality, given that they may reflect subtle aspects of the micromanipulation of specimens. We are currently developing a motorised platform to conduct self-righting tests, which when fully developed, should help addressing the chirality question.

(2.4) The genotype of the larvae used for Figure 2 experiments is missing.

Thank you for pointing this out. These were again *w¹¹¹⁸* larvae; this detail has now been added to the figure legend and the main text.

(2.5) The experiment shown in Figure 2E-G reports the proportion of larvae exhibiting self-righting behavior. Is the self-righting speed comparable to that measured using the setup in Figure 1?

Thank you for pointing this out. We have now added average self-righting times to the figure legends of figures 1 and 2. The self-righting times across for the dorsal + ventral contact conditions was notably longer than dorsal-only cases, which were also slightly longer than the “standard” case. This is perhaps to be expected, as the larvae are encountering unusual and ambiguous situations. We suggest the extra time could reflect an additional decision-making step or action flip-flopping process, or simply physical constraints on the movement (for example, not being able to use some parts of the body).

(2.6) Line 496 states: "However, the effect size was smaller than that for the entire multidendritic population, suggesting neurons other than the daIVs are important for self-righting". Although I agree that this is the more parsimonious hypothesis, an alternative interpretation of the observed phenomenon could be that the effect is not due to the involvement of other neuronal populations, but rather to stronger Gal4 expression in daIVs with the general driver compared to the specific one. Have the authors (or someone else) measured or compared the relative strengths of these two drivers?

We agree with this suggestion and to address this concern, we have added as part of our new figure Supp. Fig. S3, a dedicated panel S3C showing fluorescence measurements from ddaC using the 109(2)80-Gal4 and ppk-Gal4 lines. We found no difference in tdTomato fluorescence intensity, suggesting equal expression strength across the two Gal4 drivers. Our new results for axial daIV inhibition are also consistent with this effect size difference, further suggesting that inhibition of all md neurons poses stronger challenges for self-righting compared to the daIV neurons alone.

(2.7) Is there a way to quantify or semi-quantify the expression of the Hox genes shown in Figure 6A? Also, was this experiment performed more than once (are there any technical replicates?), or was the amount of RNA material insufficient to allow replication?

Unfortunately, we only had limited amounts of mRNA extracted from FACS-sorted 109(2)80>GFP cells to feed our reverse transcriptase reactions and used much of these samples for the experiment reported. After Rev2 suggestion we went back to our freezers, recovered traces of the samples used in the original experiment, and attempted a new amplification; despite this effort, this new experiment was unsuccessful. We feel that the main point deduced from the original experiment is valid in that we obtained amplicons of the expected size for all the Hox transcripts analysed and that for those cases in which we observed biological effects – i.e. Antp and Abd-B – we corroborated protein expression in the 109(2)80 domain using immunohistochemistry. We are currently expanding this project examining the roles of all Hox genes across the entire sensory system and shall report the expression patterns of all Hox genes in each of the subcomponents of the sensory system the future.

(2.8) Since RNAi constructs can sometimes produce off-target effects, it is generally advisable to use more than one RNAi line per gene, targeting different regions. Given that Hox genes have been extensively studied, the RNAis used in Figure 6B are likely already characterized. If this were the case, it would strengthen the data to mention it explicitly and provide references documenting the specificity and knockdown efficiency of the Hox gene RNAis employed. For example, does Antp RNAi expression in the 109(2)80 domain decrease Antp protein levels in multidendritic anterior neurons in immunofluorescence assays?

We used the TRiP RNAi lines, specifically the Valium10 selection available from the

Bloomington Stock Centre. Unfortunately, there is not much information on how specific the Hox RNAi lines are or whether they might have off-target effects.

(2.9) In addition to increasing self-righting time, does Antp downregulation also affect head casting behavior or head movement speed? A more detailed behavioral characterization of this genetic manipulation could help clarify how closely it relates to the behavioral phenotypes described in the previous experiments.

This would be an interesting line of investigation. As described in a previous comment, this is currently unfeasible for us given some important differences between experiments including larval stage and recording conditions. We have added some speculative comments to the manuscript describing the larval behaviour under Hox RNAi.

(2.10) Does down-regulation of Antp in the daIV domain also increase self-righting time?

Given the new results with axial effects of daIV neurons, we also sought to address this point with a new series of experiments expressing Hox RNAi constructs in the ppk-Gal4 domain. The new data is shown in a new figure (Figure S8 [↗](#)) displaying self-righting times for ppk-Gal4-Hox-RNAi. Interestingly, we found no effect of any RNAi expression on self-righting times, suggesting that md types other than daIVs are under Hox regulation that is important for self-righting.

Recommendations for the authors:

Reviewing Editor Comments:

The reviewers were enthusiastic about the value and quality of this study by Roseby and colleagues. There were two main issues that emerged from the reviews that we're highlighting for the authors to address, should they choose to:

(1) A little more cell-type resolution of the anterior region

The anterior region includes a lot of sensory neurons that may be contributing to the effect. Some sensory neurons (e.g., daIV) have been implicated in righting - are these the ones carrying the anterior signal? Are dorsal sensory neurons promoting righting and ventral ones stalling it?

We are not suggesting a complete sensory-neuron mapping in the anterior region. Instead, we propose the authors conduct a focused check: repeat the axial inhibition with a daIV-specific driver (same photomask assay) to show the A-P effect within the implicated class, and, if possible, replicate one key result with an alternative broad md driver to address Gal4 strength/off-target expression.

As mentioned above (see Rev1 comment) we have indeed carried out a new experiment using an alternative driver to *109(2)80-Gal4* and testing the impact of these manipulations on larval behaviour. The revised version of our MS includes a new figure Supp Fig S3 which shows self-righting times when using the *ppk-Gal4* driver with the opto-axial technique. As with the *109(2)80-Gal4* driver, self-righting was delayed in anterior but not posterior inhibition conditions, suggesting the daIV neurons specifically act in a region-specific manner to trigger postural control behaviour.

Furthermore, in another new figure, Supp Fig S7, we show that head casting behaviour is also increased in the same manner as with the *109(2)80-Gal4* driver. These new panels and figures are cited within the sub-sections entitled “Optogenetic inhibition of anterior but not posterior multidendritic neurons delays self-righting” and “Inhibition of anterior multidendritic neurons is associated with increased head casting during self-righting”, on pages 25 and 28, respectively. We are grateful to R1 for this suggestion, which we consider qualitatively improves the quality of our paper.

(2) *The Hox section to strengthen this section, we recommend:*

(a) *Confirm specificity/efficacy of knockdown (e.g., Antp protein reduction in targeted md neurons and a second RNAi line if available).*

This is a reasonable comment. For our experiments, we selected a *UAS-Antp^{RNAi}* line (Bloomington #27675) given that this construct has been: (i) utilised in several previous studies as the main and single line to interfere with Antp expression (e.g. Baek et al. 2013 Development; Paul et al. 2021 Nature Comms) and (ii) shown to display a consistent reduction in Antp protein levels of approximately 50% (see Poliacikova et al. 2024 Science Adv.). Furthermore, previous work comparing #27675 with other *UAS-Antp^{RNAi}* lines has demonstrated that all available lines lead to a similar level of reduction in protein expression, although the #27675 line exhibits the most consistent effects (lower variability) (Poliacikova et al. 2024 Science Adv.). Unfortunately, at this point in time, we do not have the capacity to conduct new experiments with other RNAi lines, but consider that the information and arguments mentioned above should be reassuring about our choice of a reasonable and previously validated method to interfere with Antp expression.

(b) *Perform one temporal control (GAL80^{ts}) or a simple rescue, to separate developmental vs acute roles.*

This is a good and interesting suggestion, but we consider that the discrimination between developmental and physiological effects falls outside the scope of this study. Indeed, experiments of this kind are currently being conducted in our lab as part of a wider examination of Hox gene roles in the sensory system.

(c) *Place the results clearly in the context of prior work (e.g., Parrish 2007), so the mechanism isn't left hanging.*

This is an important point, and we have now done this. Many thanks for pointing this out.

Reviewer #1 (Recommendations for the authors):

(1.1) *A Gal4 line for the pannier dorsal specification gene shows expression in dorsal sensory neurons, as described in Galindo et al., Development, 2023, and could help tease apart dorsal v. ventral contributions.*

This is an interesting suggestion. However, we understand that the *pannier (pnr)* Gal4 line mentioned in Galindo et al. 2023 is an enhancer trap inserted in the *pnr* locus which drives expression in neural as well as non-neural tissues such as the embryonic dorsal ectoderm (see: Calleja et al. 1996 Development; Stronach et al. 2014 Genetics). Although, as Rev1 rightly indicates, this line also labels dorsal cluster sensory neurons, including ddaC (cIV) and ddaF (cIII) neurons the fact that the line displays expression in non-neural tissues makes its use in behavioural experiments difficult as non-neural effects might affect the behavioural patterns studied. A possible way to instrument the *pnrGal4* tool into behavioural analyses might involve the creation of the necessary variants to implement a split-Gal4 approach, but this, we believe, unfortunately falls out of the scope of this study.

(1.2) Potential roles for *daII* neurons and *daI* neurons are not examined. Drivers have been described for *daII* neurons, and there are drivers that will target a majority of proprioceptive *md* neurons, so these could be examined to complete the analysis started here.

This is another interesting suggestion by Rev1, but we consider that the fine-grain mapping of effects mediated by sensory neuron sub-classes falls outside the scope of this study aimed at mapping sensory regional effects on self-righting. This does not take the merit of the suggestion away, and indeed, experiments of this kind are currently being conducted in our lab as part of a comprehensive examination of Hox gene roles in the sensory system.

(1.3) To account for 109(2)80 off targets, the authors could consider other lines that silence most or all *md* neurons (*clh201-Gal4*; *5-40-Gal4*; *21-7-Gal4*) that could at least have different central offtargets. Some other lines are broad somatosensory system drivers but sensory-specific (*pebbledGal4*).

This is an interesting comment, and so are the suggestions made. Although to include this kind of verification would be interesting, when carrying out our experiments, we did not observe any central expression at all. Also, to repeat all our experiments in which we use the established and validated 109(2) 80 line using instead these four Gal4 lines, is unfortunately out of scope for us at this point in time. We will nonetheless consider these comments by Rev1 in future extensions of our work.

(1.4) There is a typo on line 481; it should be "other".

We are grateful to R1 for pointing this out. This has now been amended

Reviewer #2 (Recommendations for the authors):

(2.1) Lines 91-92 cite references describing self-righting behavior across different animal groups, which is illustrated in Figure 1B. It would be helpful to indicate these references directly in the figure. For example, instead of using dots to denote their presence (which are, in a way, redundant since the behavior is reported in all groups), numbers or letters could be used to refer to the specific papers describing them.

Thank you for this suggestion. We have now replaced the original dots by an abridged citation of a key paper providing evidence in that specific animal group, e.g. Smith, et al. 1997; Rogers et al. 2015

(2.2) In Figure 1A, the diagrams illustrate the two large dorsal tracheae, which nicely indicate the larva's orientation. However, since they are drawn in a very light gray, they can be difficult to distinguish without zooming in. It might improve clarity if the tracheae were made slightly more prominent.

Thank you for this suggestion. We have now implemented this change.

(2.3) In Figure 1E, the dotted line and green bar mark the segment of the recording corresponding to self-righting, which is then quantified in Figure 1G. Was the same procedure applied when analyzing tail speed, or was it limited to head speed? Figure 1F does not show a dotted line or green bar, which is confusing; it would be helpful to clarify the reason for this discrepancy. Also, in Figure 1G, there is an inset showing photos of the movement sequence with the green bar and the caption 'Trimmed to SR sequence,' which implies to me that for tail speed, the 0.75-1 segment of the recording was also used for quantification. I suggest adding the dotted line and green bar to Figure 1F and removing this inset from Figure 1G, as it appears quite small and disrupts the layout of the figure. If it is retained, the figure legend should explicitly refer to the inset.

Thank you for pointing this out. We have amended these figures as suggested.

(2.4) In Figures 1 and 2, the box plots include the individual data points, whereas Figures 3 and S2 do not. For data transparency, it would be important to show the individual measurements here as well. I strongly recommend adding them to the figure, or alternatively providing a clear rationale in the text for not doing so.

Thank you for mentioning this. The reason data points are not shown in Fig 3 or S2 is because the variance extends the scale and compresses the box making it illegible. To make this clear we now explain this in the figure legends.

(2.5) In Figures 4 and 5, the distribution of self-righting times from the optogenetic inhibition experiments is shown using bar graphs rather than box plots, as in the previous figures. This choice obscures the data distribution, since all bars reach down to zero. Replacing the bar graphs in Figures 4 and 5 with box plots would more clearly convey the experimental results.

We thank Rev2 for this comment, which gives us an opportunity to clarify the matter. Distributions of SR times are drawn with bars because we compare means +/- variance in the analysis, and not medians +/- IQR as is done in the other experiments. The choice of visualisation reflects the analysis, which is what is recommended by statisticians. Plus, we also show the individual observations, meaning the distribution can be observed. We hope that it is now clear that we are not obscuring any distributions.

(2.6) Figure 6 would benefit from some reorganization. Panel A is very small and dense with information, making it difficult to interpret without significant zooming. In particular, the FACS graph is nearly impossible to read, as the axes remain unclear even when enlarged. It might be best to either remove this graph and replace it with a cartoon version of FACS-sorted populations, and reorganize the figure to ensure legibility. Additionally, the current layout progresses from the bottom up, which takes time to follow. Comprehension could be improved if the sequence began with the larva dissection placed in the top left area of the figure, where readers typically look first (I appreciate that this is mentioned in the figure legend; however, a different layout might present the information more effectively).

We appreciate the constructive spirit of this comment and have indeed considered Rev2 suggestions including drafting new layouts of this figure. After all this experimentation, we remain of the view that the original presentation is probably the best trade-off between size and clarity, offering more space for the appreciation of confocal imaging and its interpretation.

Minor corrections:

*(1) Throughout the text, the word *Drosophila* appears sometimes in italics and sometimes in regular font; please standardize its formatting for consistency.*

Amended

(2) Line 179: the use of three hyphens in the sentence "minimum --- in all cases < 30 s --- to avoid larval desiccation" is unusual; exchanging them for commas or brackets is advised.

Amended

(3) Line 183: in w1118, the numbers are usually in superscript (not subscript), and the w should be italicized.

Amended

| (4) In line 783, there is an incorrect space between "is" and the comma in "...repertoire, which is , in...".

Amended

| (5) In Figure 2G, the left panel appears partially cut off, which makes the text at the edges difficult to read. It might help to adjust the panel so that all labels are fully visible.

Done

| (6) In the current version of the manuscript, Figure 5 is presented before Figure 4, which is confusing.

This has been amended.

| (7) Two videos are included in the supplementary material, but I could not find any reference to them in the main text of the manuscript.

This has been amended.

<https://doi.org/10.7554/eLife.108505.2.sa0>